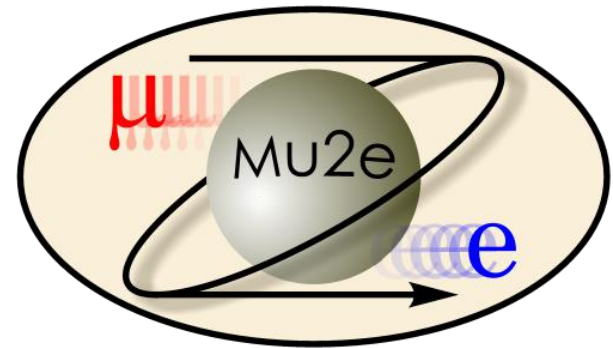


# The Mu2e Experiment at Fermilab



---

STEVEN BOI, UNIVERSITY OF VIRGINIA  
*ON BEHALF OF THE MU2E COLLABORATION*  
*NUFACT 2018*

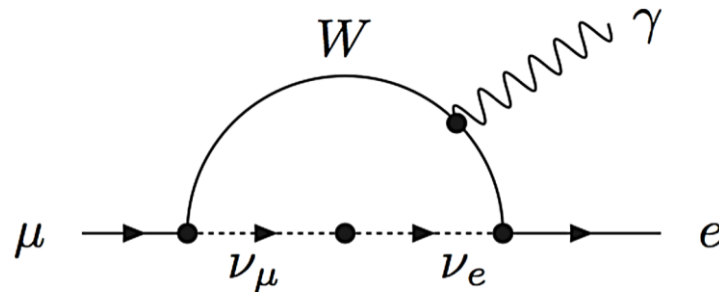


# Charged Lepton Flavor Violation and the SM

In an extension of the standard model, one which includes neutrino oscillations, lepton flavor is only approximately conserved, with some charged lepton flavor violation (CLFV) occurring due to neutrino oscillations.

Such a process is exceedingly rare, a rate too small to be observed.

*Bonus:* since we will never observe this, it is not a background to CLFV searches.

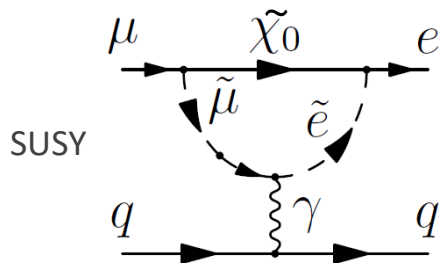


$$\text{BR}(\mu \rightarrow e \gamma) = \frac{3\alpha}{32\pi} \left| \sum_{i=2,3} U_{\mu i}^* U_{ei} \frac{\Delta m_{1i}^2}{M_W^2} \right|^2 < 10^{-54}$$

# CLFV beyond the SM

While CLFV within the SM is effectively unobservable, the rate of  $\mu + N \rightarrow e + N$  is uniquely sensitive to a host of BSM physics.

- Observation of  $\mu \rightarrow e$  conversion is an unambiguous sign of new physics.
- Easy to produce high intensity muon beams.
- BSM models predict effects that would be measurable by next-generation experiments.



★★★
Large effects
★★
Small effects
★
No effects

Flavor physics effects for the most interesting observables in a selection of SUSY and non-SUSY models.

	AC	RVV2	AKM	$\delta$ LL	FBMSSM	LHT	RS
$D^0 - \bar{D}^0$	★★★	★	★	★	★	★★★	?
$\epsilon_K$	★	★★★	★★★	★	★	★★	★★★
$S_{\psi\phi}$	★★★	★★★	★★★	★	★	★★★	★★★
$S_{\phi K_S}$	★★★	★★	★	★★★	★★★	★	?
$A_{CP}(B \rightarrow X_s \gamma)$	★	★	★	★★★	★★★	★	?
$A_{7,8}(B \rightarrow K^* \mu^+ \mu^-)$	★	★	★	★★★	★★★	★★	?
$A_9(B \rightarrow K^* \mu^+ \mu^-)$	★	★	★	★	★	★	?
$B \rightarrow K^{(*)} \nu \bar{\nu}$	★	★	★	★	★	★	★
$B_s \rightarrow \mu^+ \mu^-$	★★★	★★★	★★★	★★★	★★★	★	★
$K^+ \rightarrow \pi^+ \nu \bar{\nu}$	★	★	★	★	★	★★★	★★★
$K_L \rightarrow \pi^0 \nu \bar{\nu}$	★	★	★	★	★	★★★	★★★
$\mu \rightarrow e \gamma$	★★★	★★★	★★★	★★★	★★★	★★★	★★★
$\tau \rightarrow \mu \gamma$	★★★	★★★	★	★★★	★★★	★★★	★★★
$\mu + N \rightarrow e + N$	★★★	★★★	★★★	★★★	★★★	★★★	★★★
$d_n$	★★★	★★★	★★★	★★	★★★	★	★★★
$d_e$	★★★	★★★	★★	★	★★★	★	★★★
$(g-2)_\mu$	★★★	★★★	★★	★★★	★★★	★	?

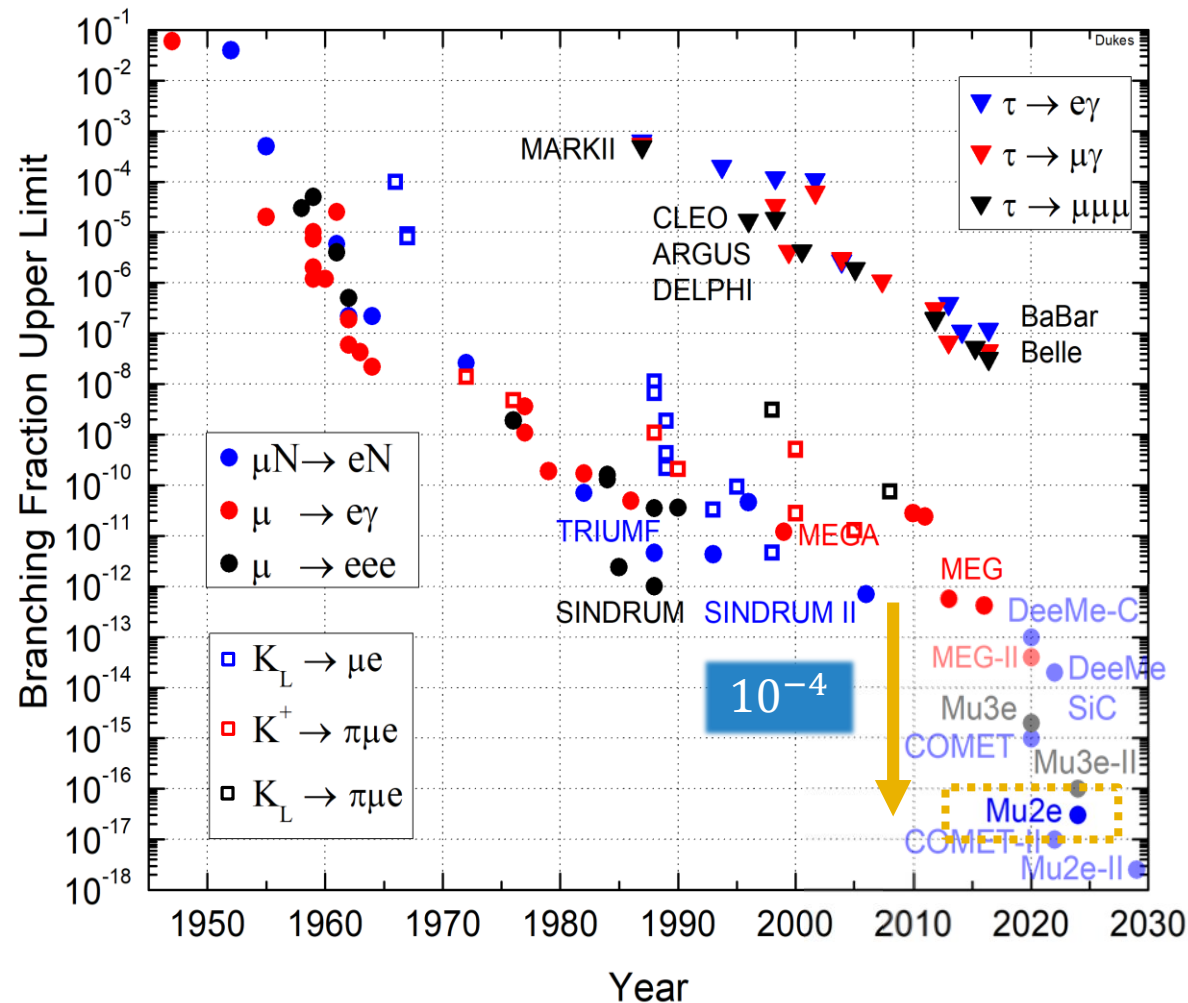
A. de Gouvêa, et al

# Historical CLFV Searches

Since the 1940s, searches for CLFV have been made, but so far only tighter constraints have been placed.

Next-generation experiments will explore unconstrained phase space favored by many BSM models.

Mu2e intends to improve the sensitivity by four orders of magnitude over the present limit.



# $\mu + N \rightarrow e + N$

A simplified CLFV Lagrangian:

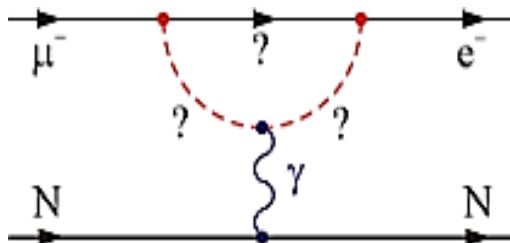
$$\mathcal{L}_{CLFV} = \frac{m_\mu}{(1 + \kappa)\Lambda^2} \bar{\mu}_R \sigma_{\mu\nu} e_L F^{\mu\nu} + \frac{\kappa}{(1 + \kappa)\Lambda^2} \bar{\mu}_L \gamma_\mu e_L \sum_{q=u,d} \bar{q}_L \gamma_\mu q_L$$

## Magnetic Moment Type Operator

Sensitive to:

$$\mu \rightarrow e\gamma$$

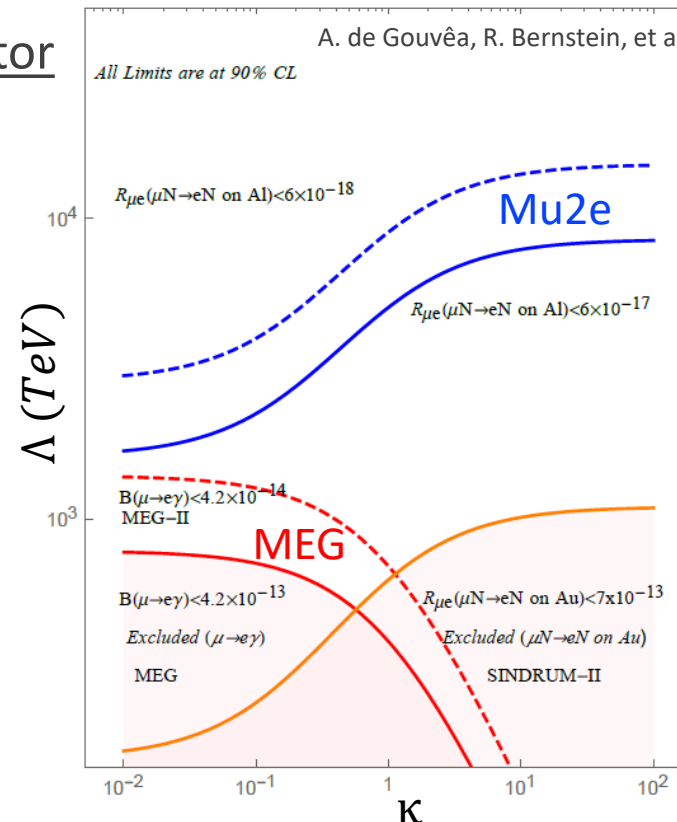
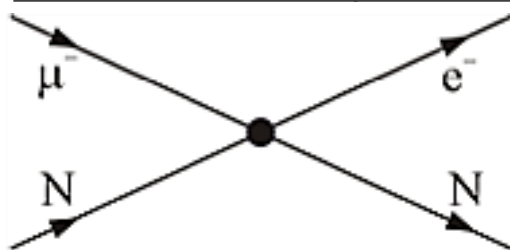
$$\mu \rightarrow e$$



## Contact Term Operator

Sensitive to:

$$\mu \rightarrow e$$



$\Lambda$ : Mass Scale

Indirect probing  
of mass scales up  
to  $10^4$  TeV.

$\kappa$ : relative  
strength of  
magnetic moment  
type and contact  
terms

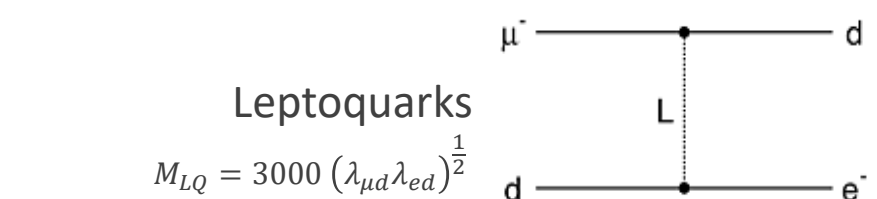
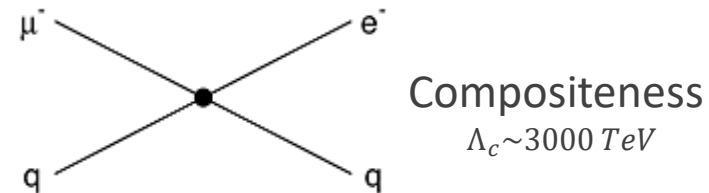
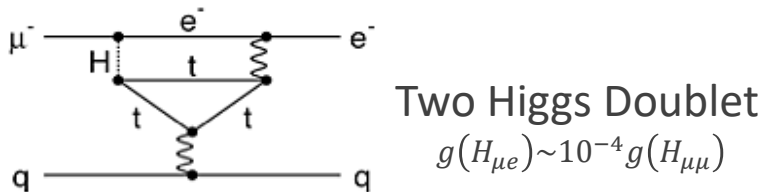
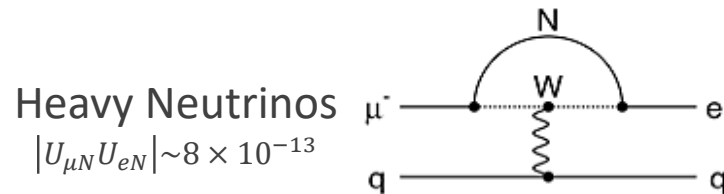
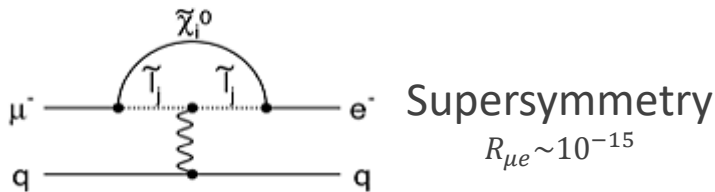
# $\mu + N \rightarrow e + N$

A simplified CLFV Lagrangian:

$$\mathcal{L}_{CLFV} = \frac{m_\mu}{(1 + \kappa)\Lambda^2} \bar{\mu}_R \sigma_{\mu\nu} e_L F^{\mu\nu} + \frac{\kappa}{(1 + \kappa)\Lambda^2} \bar{\mu}_L \gamma_\mu e_L \sum_{q=u,d} \bar{q}_L \gamma_\mu q_L$$

MAGNETIC MOMENT TYPE  
OPERATOR

CONTACT TERM OPERATOR



# $\mu + N \rightarrow e + N$ & Mu2e

Mu2e will search for the coherent, neutrino-less  $\mu \rightarrow e$  conversion in the presence of an aluminum nucleus.

$$\mu^- + (A, Z) \rightarrow e^- + (A, Z)$$

The signal is a monoenergetic electron:

- $E_e \approx m_\mu - E_b - E_{recoil} \approx 104.97 \text{ MeV}$
- Signal can be distinguished from background

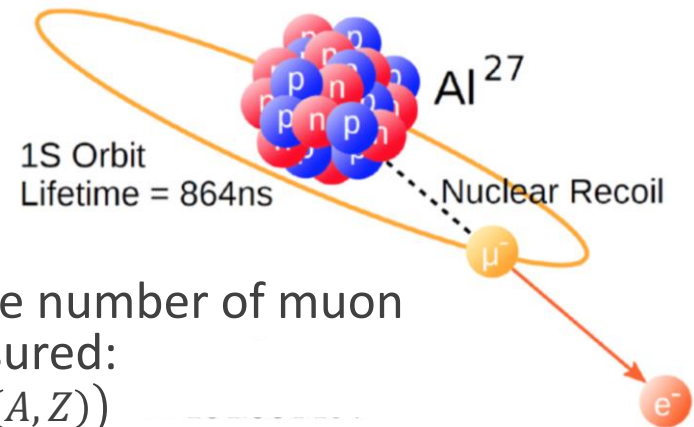
The ratio of  $\mu + N \rightarrow e + N$  conversions to the number of muon captures by the aluminum nuclei will be measured:

$$R_{\mu e} = \frac{\Gamma(\mu^- + (A, Z) \rightarrow e^- + (A, Z))}{\Gamma(\mu^- + (A, Z) \rightarrow \nu_\mu + (A, Z - 1))}$$

Mu2e intends to surpass the current limit in sensitivity by 4 orders of magnitude.

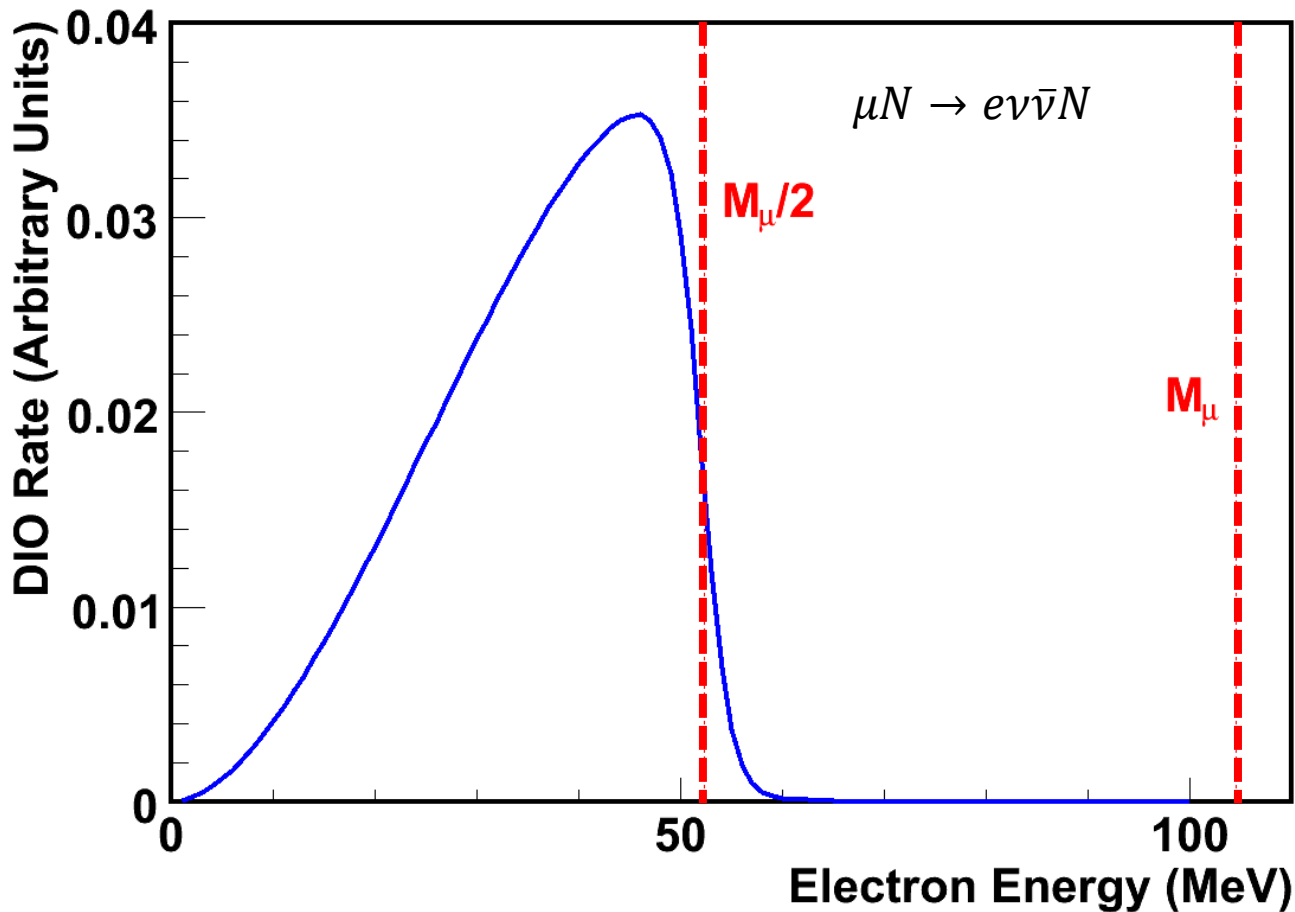
- Indirect probing of mass scales  $\sigma(10^4 \text{ TeV})$

A single event sensitivity (SES) of  $3 \times 10^{-17}$  is required.



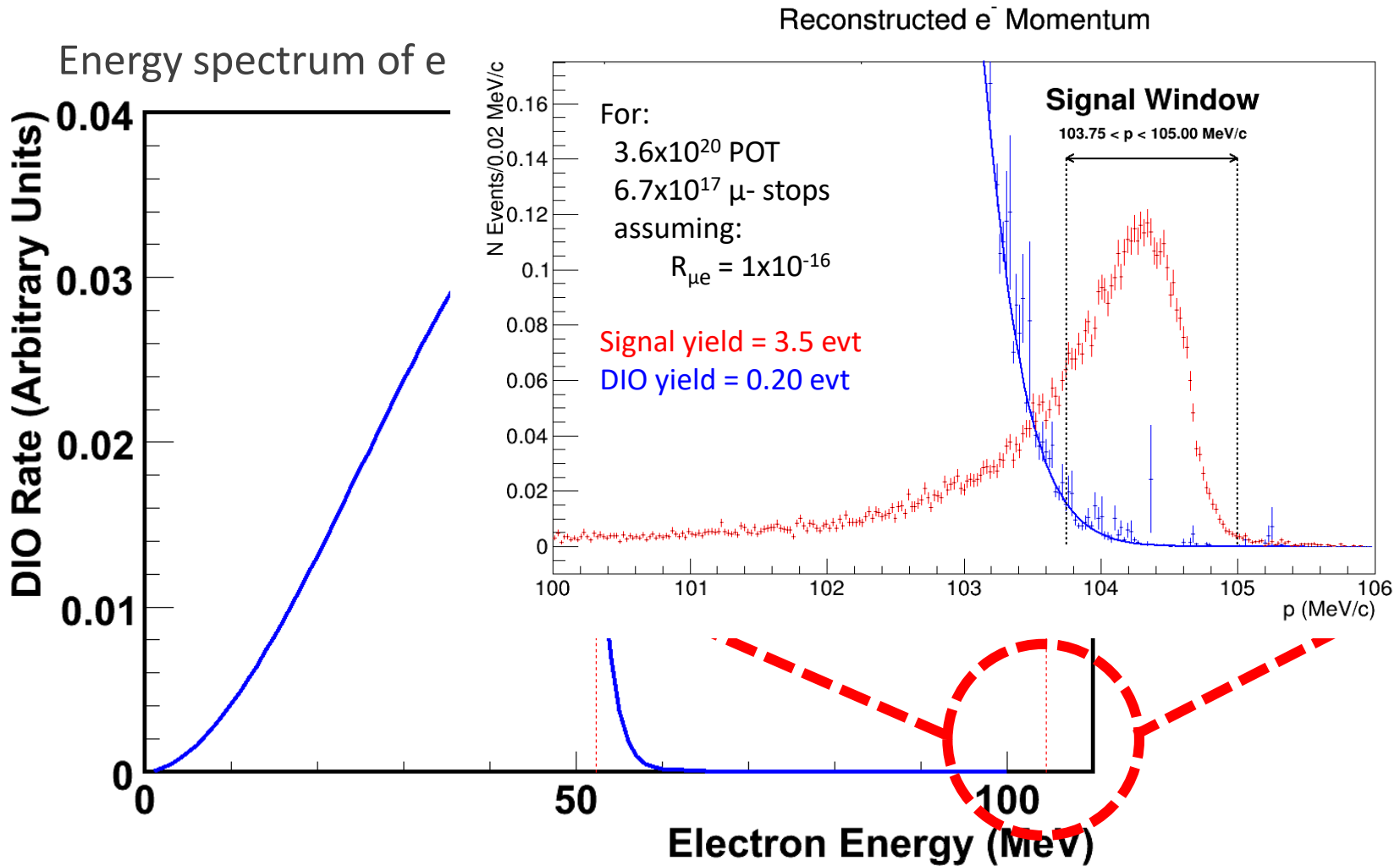
$$\mu + N \rightarrow e + N \text{ \& Mu2e}$$

Energy spectrum of electron emitted by muon decay in orbit





$$\mu + N \rightarrow e + N \text{ \& Mu2e}$$



# $\mu + N \rightarrow e + N$ & Mu2e

---

## Intent:

- Four order of magnitude improvement in sensitivity over the current limit
  - Set by SINDRUM II for  $\mu + N \rightarrow e + N$
  - Probing of mass scales up to  $10^4$  TeV

## Achievements:

- World's highest intensity muon beam
  - Graded magnetic fields for greater muon collection
- Sub-event level management of backgrounds
  - Pulsed beam structure
  - High-efficiency Cosmic Ray Veto detector
  - Tracker blind to >99% muon decay in orbit spectrum
  - Fast timing Calorimeter with good energy resolution

# The Mu2e Experiment

---

( AT FERMILAB )

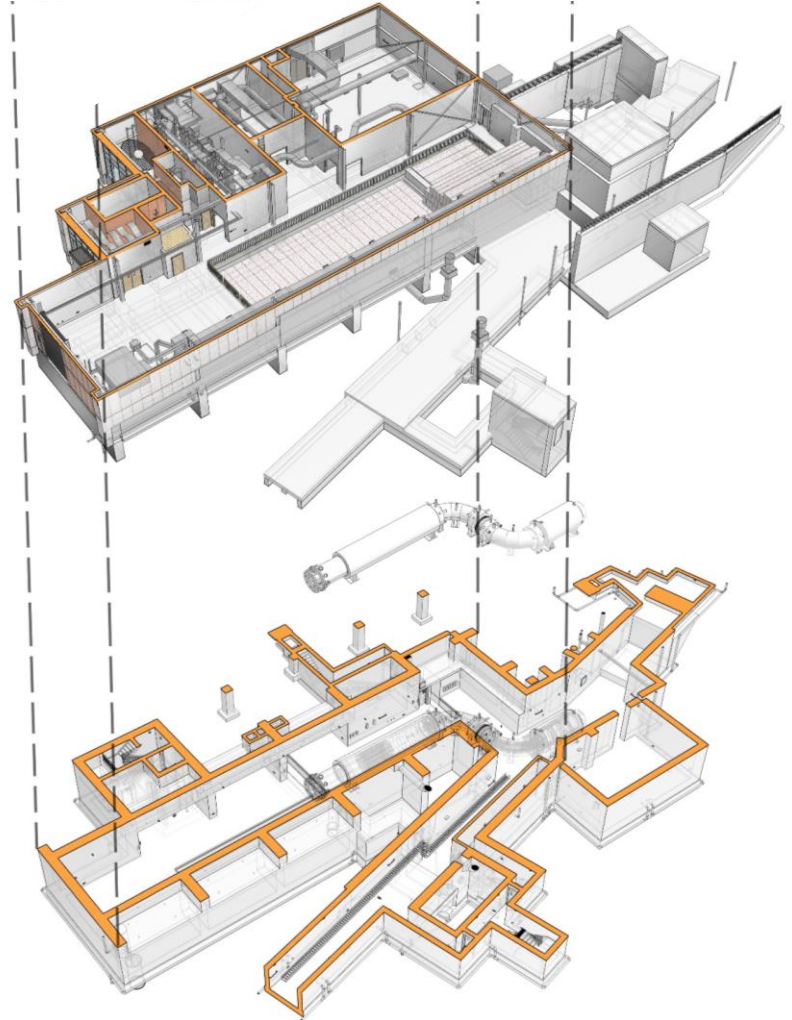
# Mu2e Collaboration

Comprised of 229 members from 37 Institutions.





# Mu2e at Fermilab



# Mu2e Beamline

Using the existing accelerator infrastructure, Mu2e will be the second building in the “Muon Campus” at Fermilab.

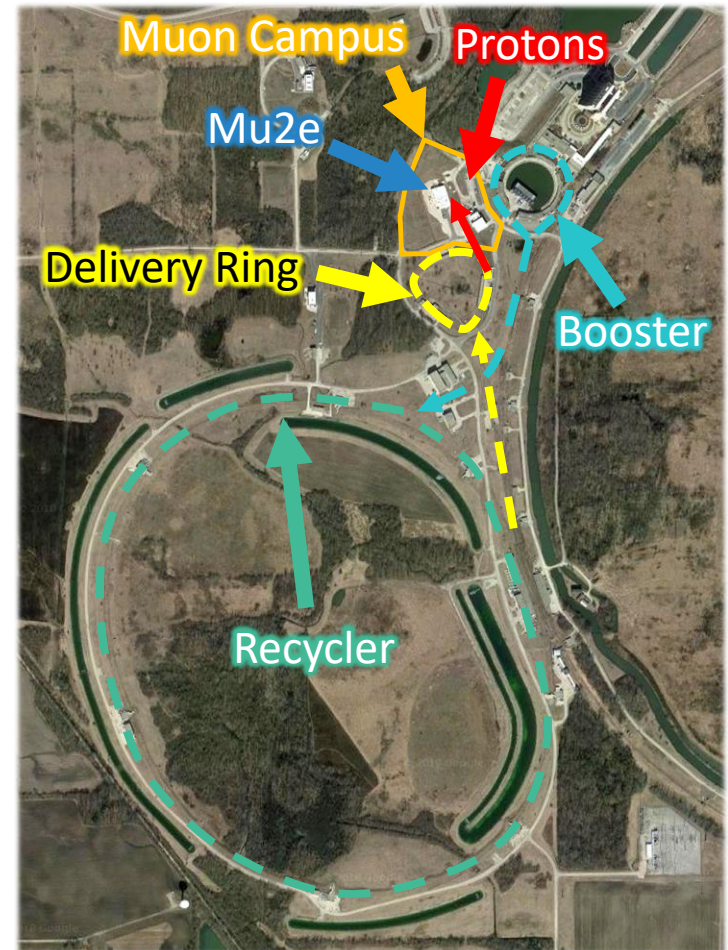
**Booster** provides 8 GeV protons to the **Recycler**.

**Recycler** stacks protons into 4 bunches.

**Delivery Ring** takes 1 out of every 4 bunches from the **Recycler**.

**Mu2e** slow-extracts **Protons** every 1695ns.

Runs with minimal impact on NOvA.

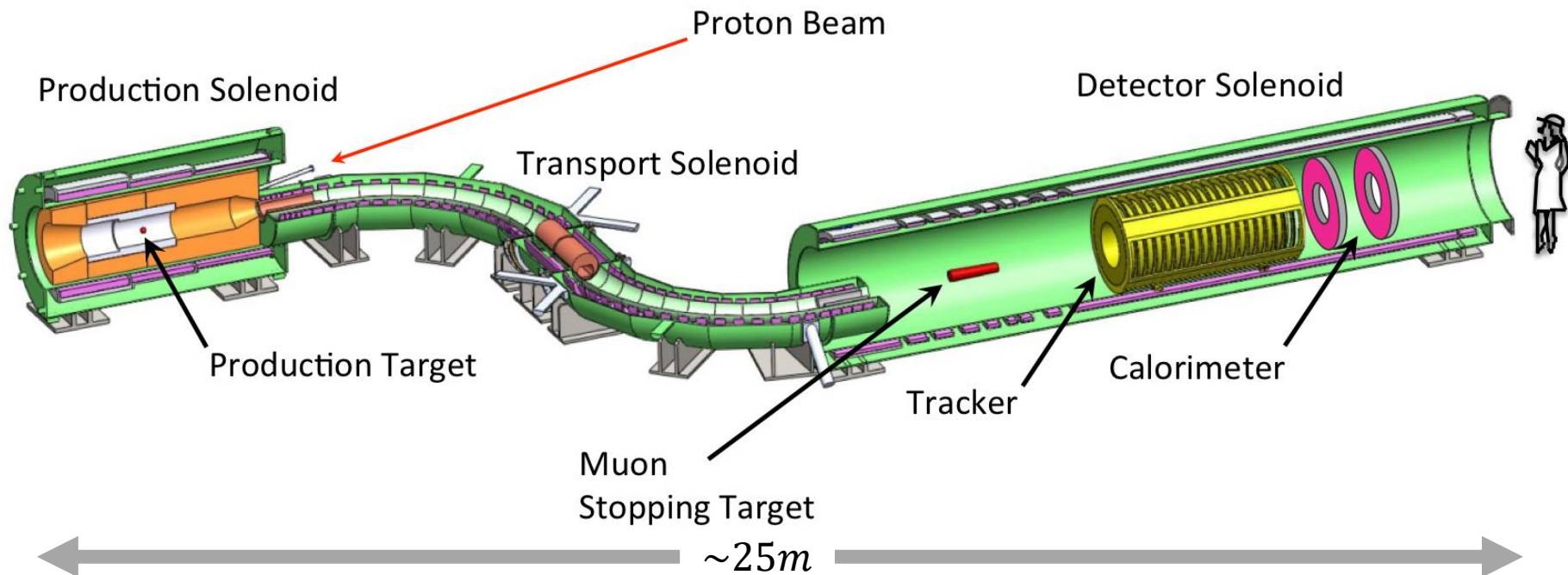




# Mu2e Apparatus

The Mu2e Apparatus is divided into three major solenoids:

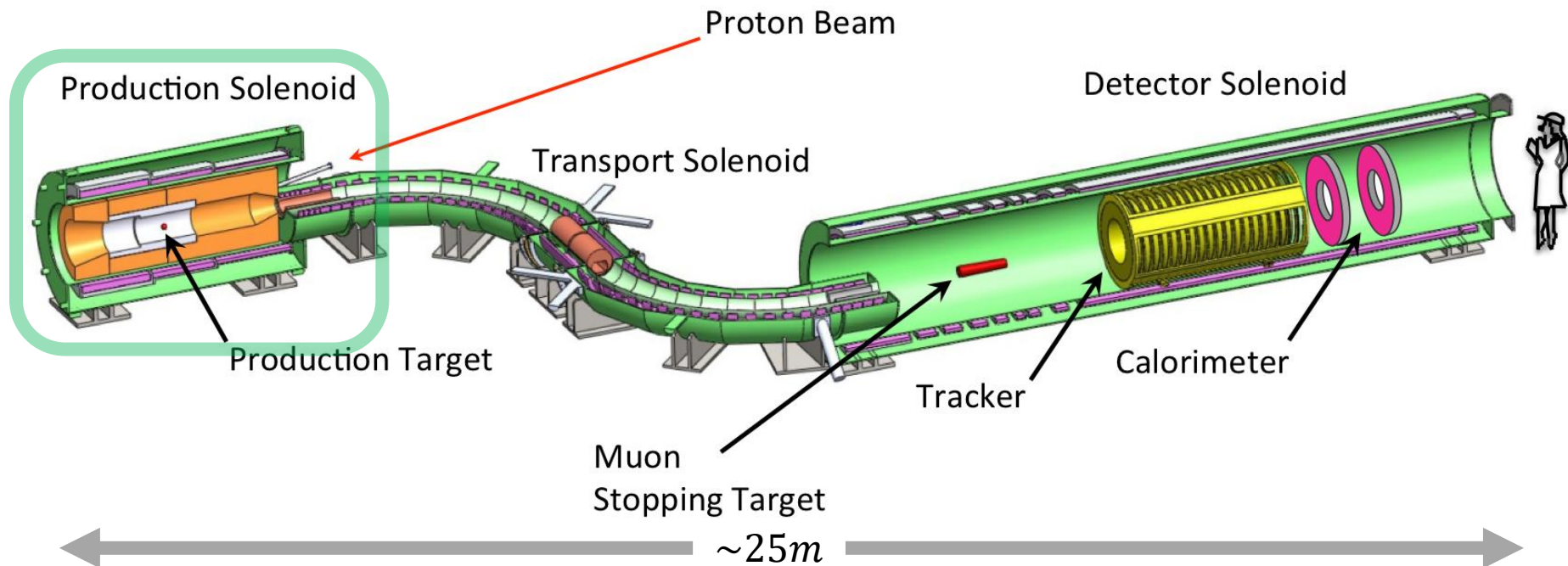
- Production Solenoid
- Transport Solenoid
- Detector Solenoid



# Mu2e Apparatus

The Mu2e Apparatus is divided into three major solenoids:

- **Production Solenoid**
- Transport Solenoid
- Detector Solenoid

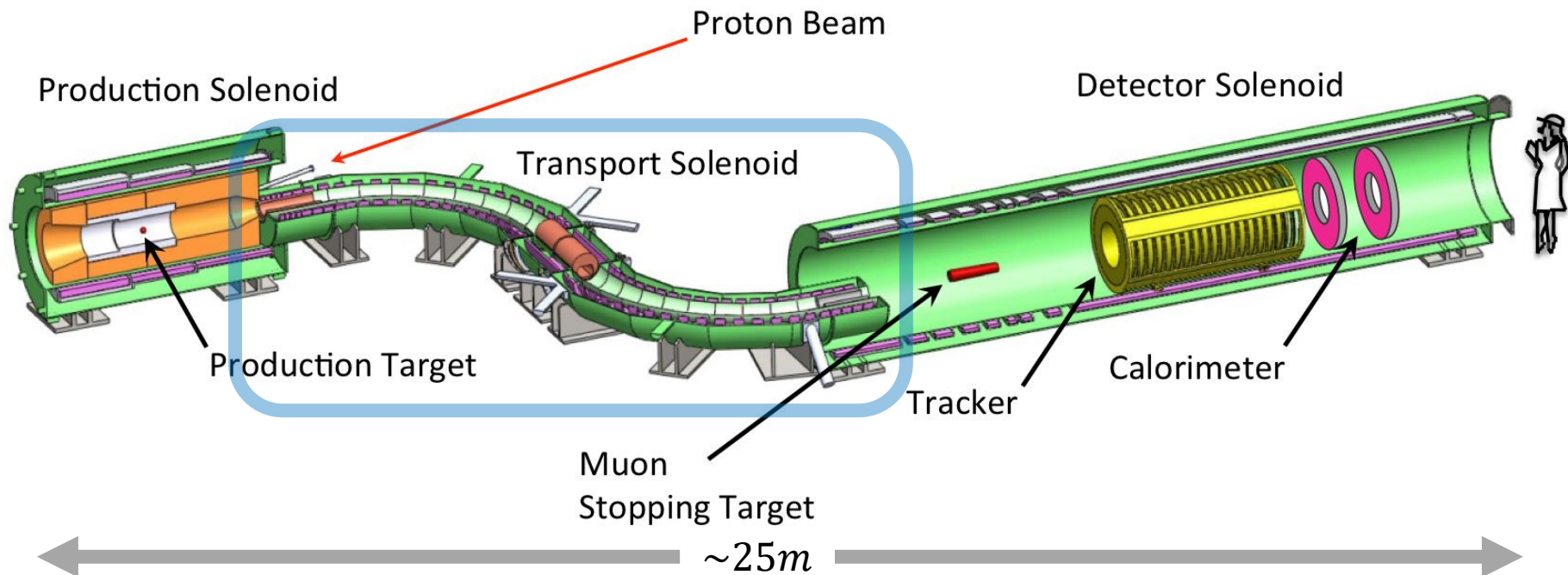




# Mu2e Apparatus

The Mu2e Apparatus is divided into three major solenoids:

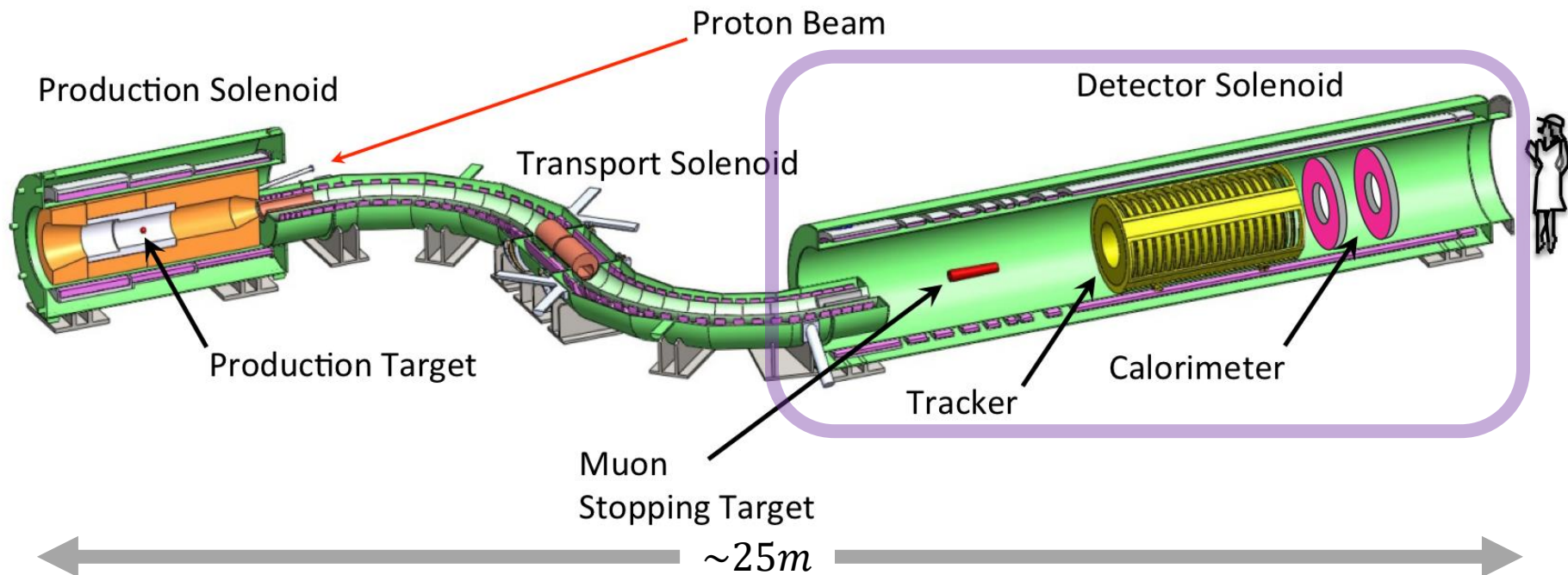
- Production Solenoid
- **Transport Solenoid**
- Detector Solenoid



# Mu2e Apparatus

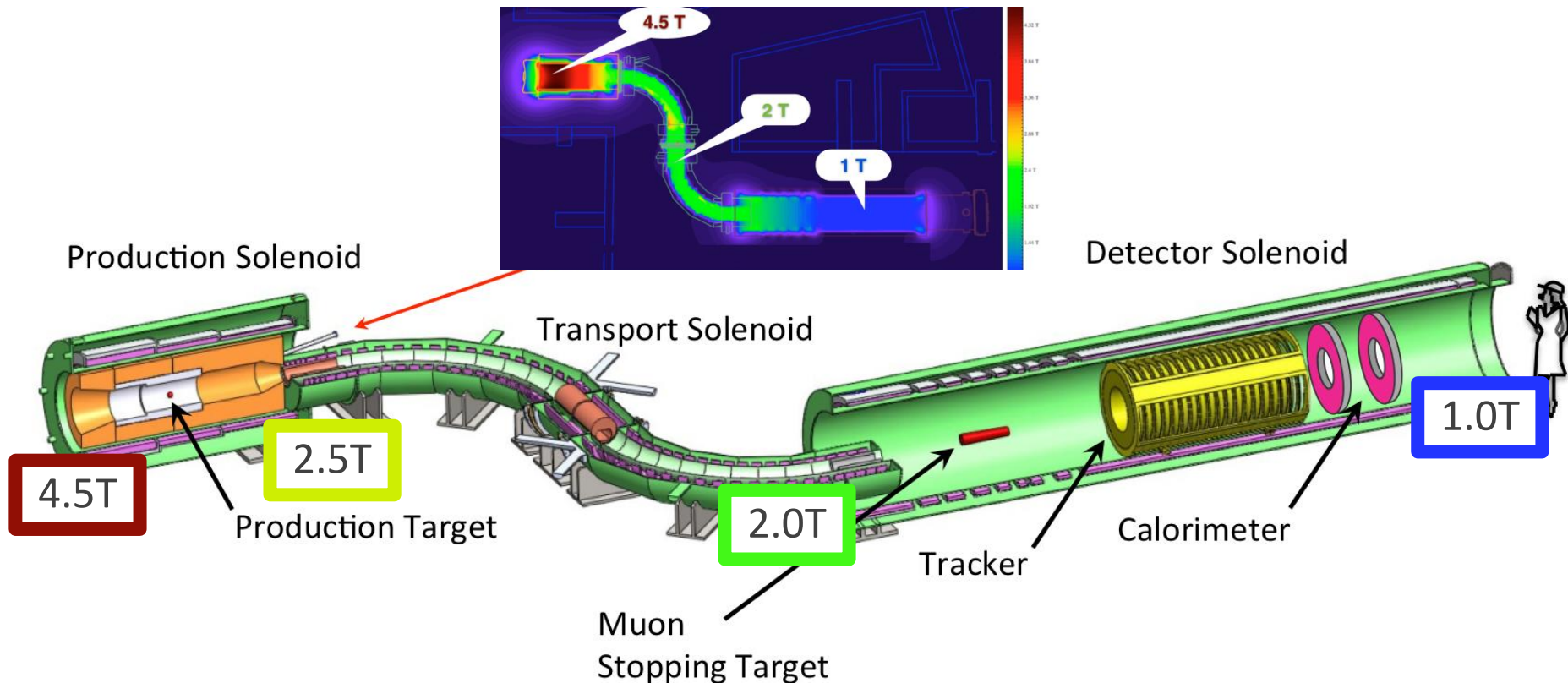
The Mu2e Apparatus is divided into three major solenoids:

- Production Solenoid
- Transport Solenoid
- **Detector Solenoid**



# Mu2e Apparatus

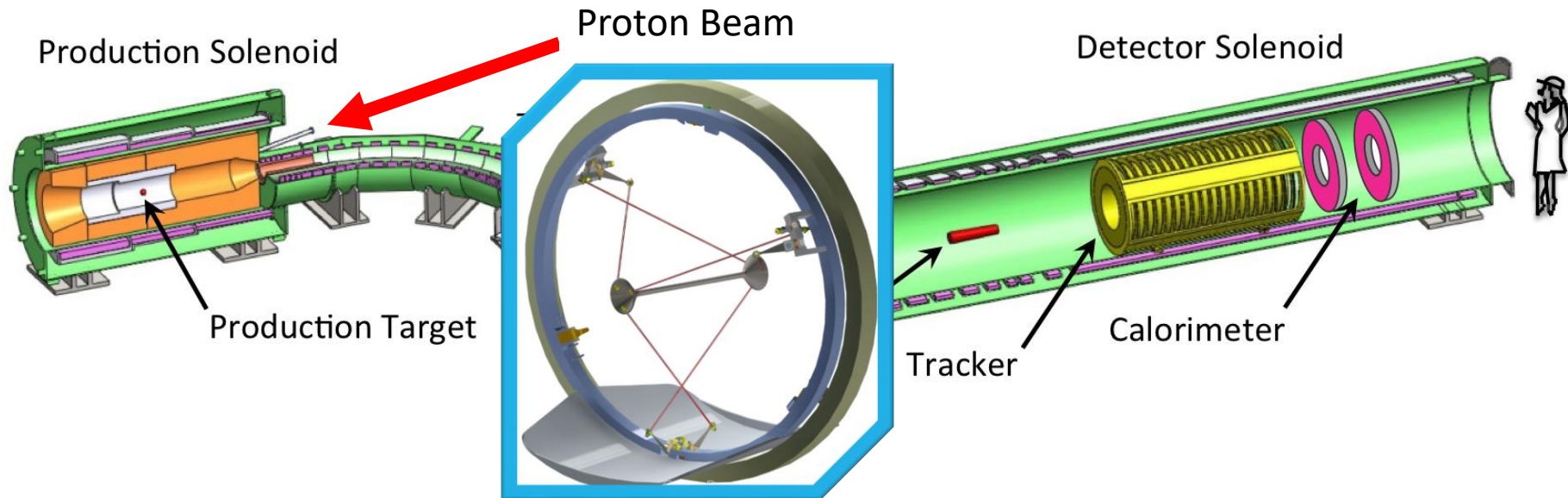
Graded magnetic fields sweep particles into the detector solenoid, creating the highest intensity muon beam to date.



# Mu2e Apparatus Production Solenoid

A proton beam incident on a tungsten production target produces  $\pi^-$ .

- 8 GeV beam with 1695ns between pulses, well timed to  $\tau^{Al} = 864\text{ns}$
- $6 \times 10^{12}$  protons/second  $\rightarrow 10^{10}$  stopped  $\mu^-$ /second
- $\pi^-$  move toward the transport solenoid, decaying into  $\mu^-$ .

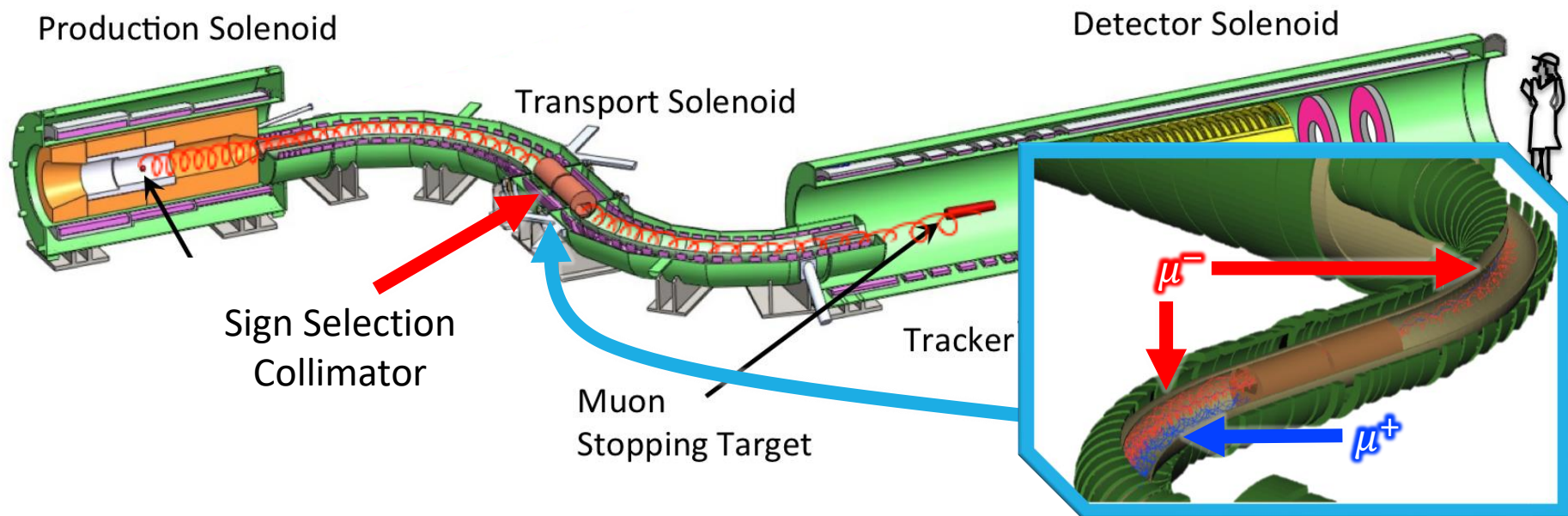




# Mu2e Apparatus Transport Solenoid

$\pi^-$  and  $\mu^-$  beam propagate through the transport solenoid (TS) to the detector solenoid.

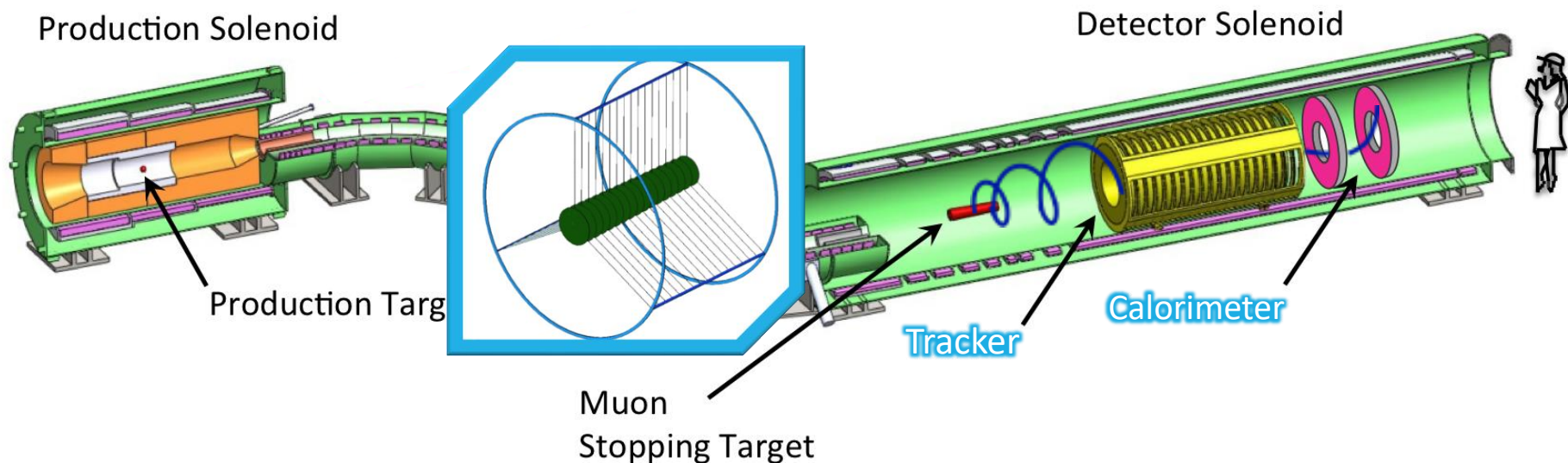
- Momentum selection
- Sign selecting collimator in the middle of the TS.



# Mu2e Apparatus Detector Solenoid

$\mu^-$  stop in an Aluminum target comprised of 37 thin 100 $\mu\text{m}$  foils.

- With a rate of  $6 \times 10^{12}$  protons/second incident on the production target,  $1.1 \times 10^{10}$   $\mu^-$ /second reach the stopping target.
- The momentum and energy of  $e^-$  coming out of the stopping target is measured by the **tracker** and **calorimeter**.



# Mu2e Apparatus Backgrounds

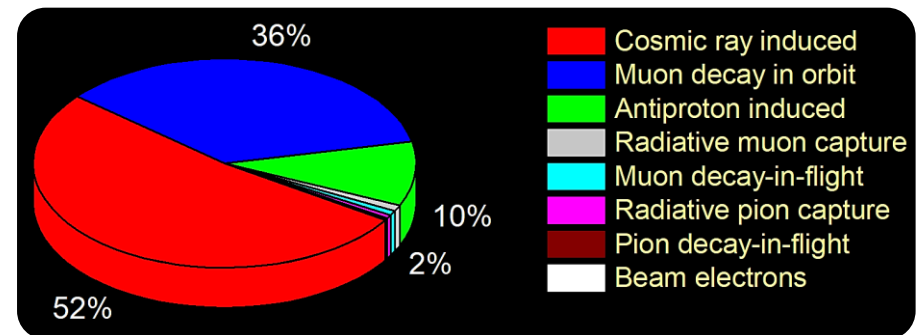
The single event sensitivity (SES) is expected to be  $3 \times 10^{-17}$ , which is around 40  $\mu \rightarrow e$  conversion events over the lifetime of the experiment (3 years) at  $R_{\mu e} = 10^{-15}$ .

For Mu2e to be a high-sensitivity experiment, the backgrounds which can mimic  $\mu + N \rightarrow e + N$  conversion must be well-understood and kept at a sub-event level.

- 0.4 events over the lifetime of the experiment.

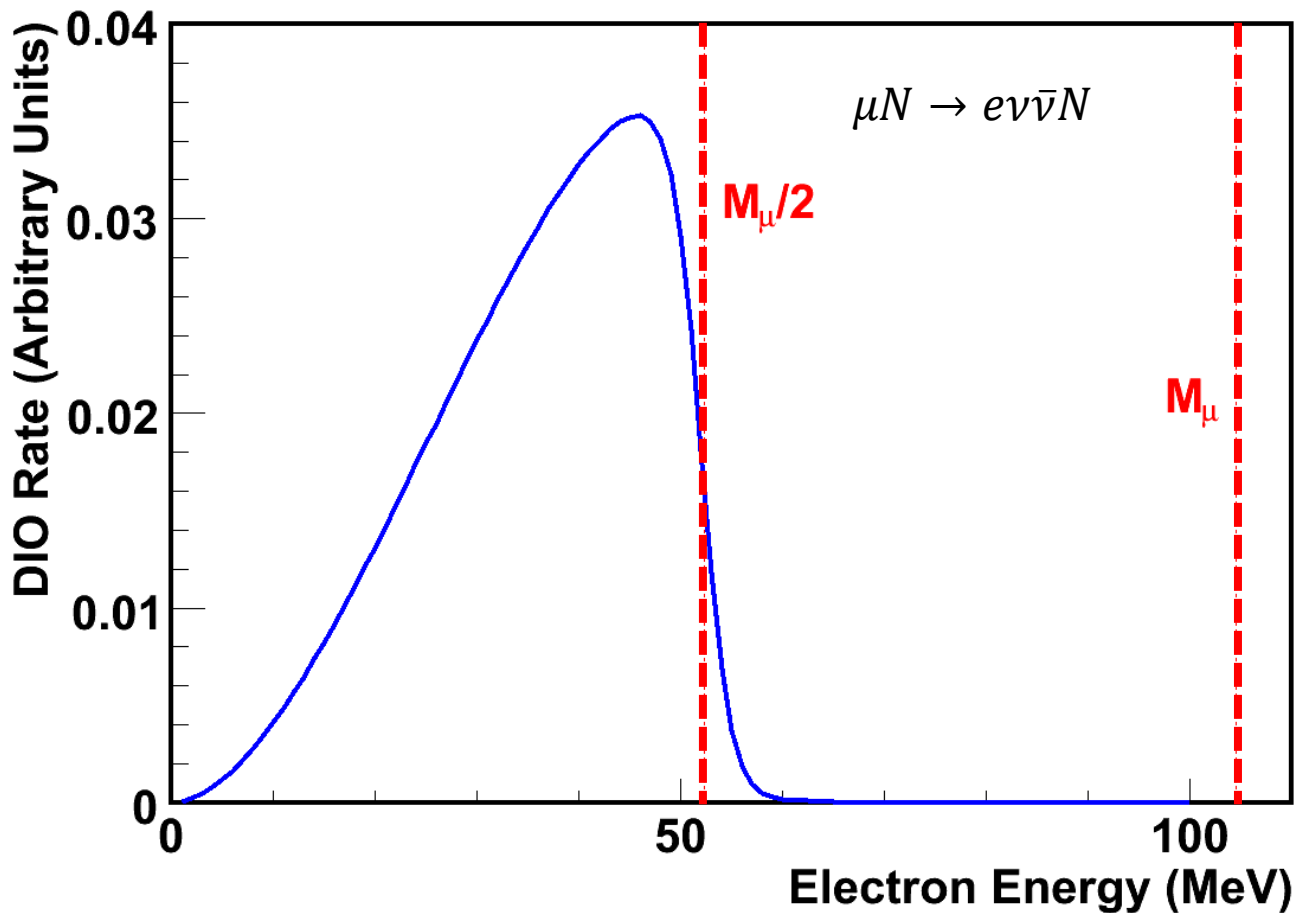
The three most prominent backgrounds for the experiment are the products of decay in orbit (DIO), anti-proton processes, with the largest background being the production of conversion-like electrons due to cosmic rays.

- Tracker and Calorimeter handles
- Cosmic Ray Veto



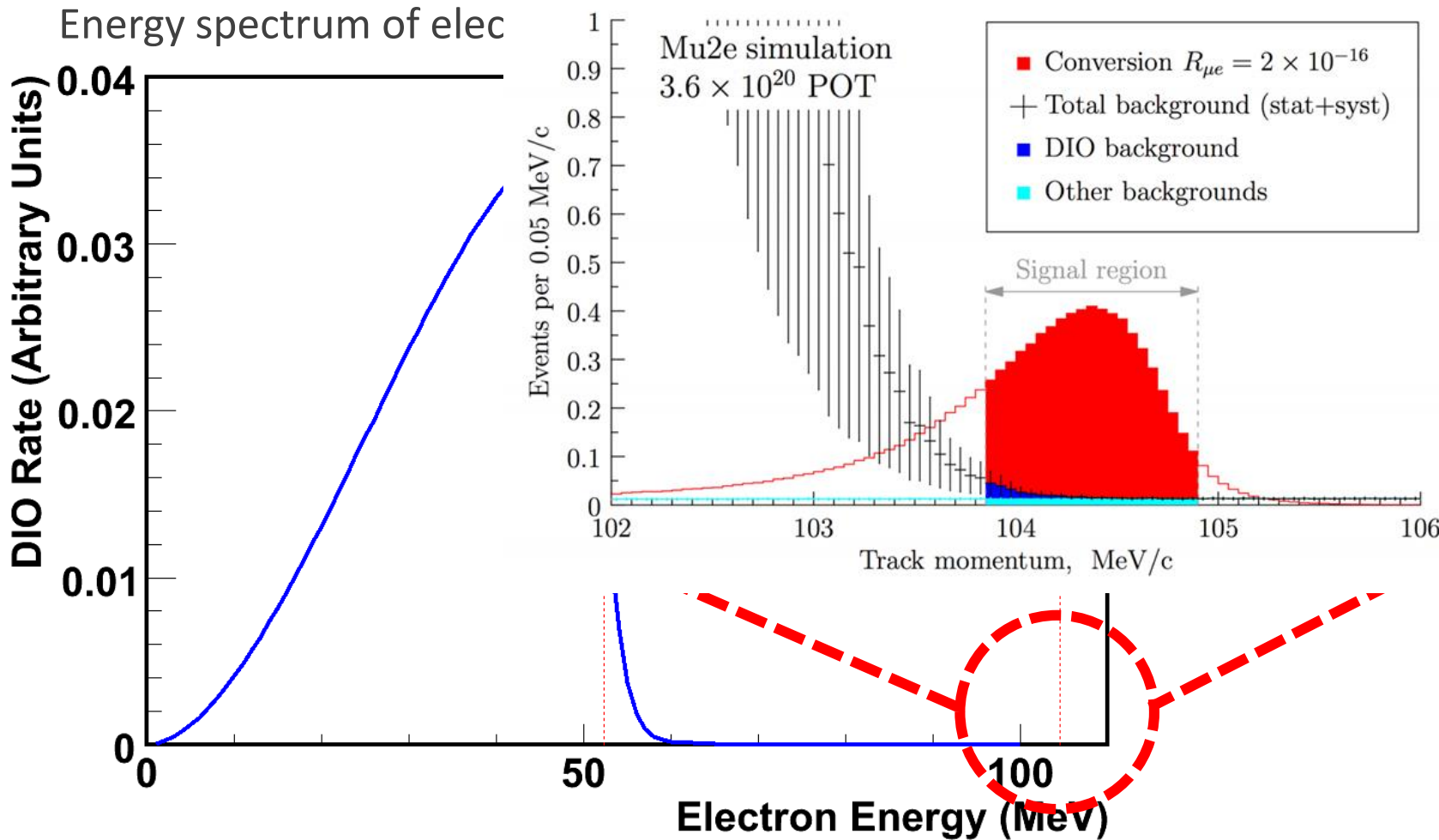
# Mu2e Apparatus Backgrounds

Energy spectrum of electron emitted by muon decay in orbit





# Mu2e Apparatus Backgrounds



# Mu2e Apparatus Backgrounds

---

Process	Expected Number
Cosmic Ray Muons	$0.25 \pm 0.026$
DIO	$0.14 \pm 0.09$
RPC	$0.025 \pm 0.003$
Antiprotons	$0.047 \pm 0.024$
Muon DIF	$< 0.003$
Pion DIF	$0.001 \pm < 0.001$
Beam Electrons	$< 5 \times 10^{-4}$
Total	$0.46 \pm 0.10$

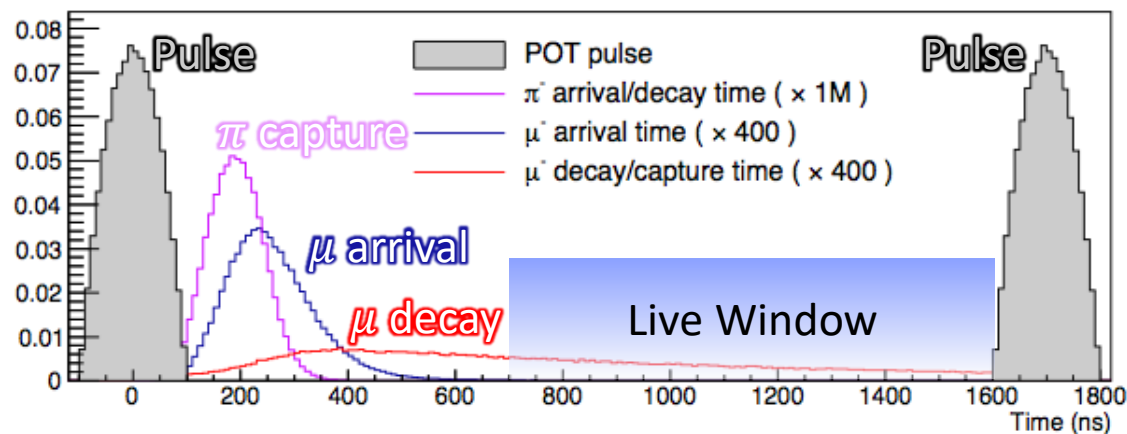
# Mu2e Apparatus Backgrounds

The live window is delayed by 700ns relative to the proton pulse.

- $\pi$  reaching and stopping in the stopping target undergo radiative pion capture (RPC). Since the live window is delayed, emission of a conversion-like electron caused by RPC is mitigated.
- Beam flash is prompt, but can blind detector components.

Protons arriving out of time with respect to the pulses must be kept to a minimum.

- Can generate additional  $\pi, \mu$  which can fake  $\mu + N \rightarrow e + N$
- Require  $10^{-10}$  out-of-pulse/in-pulse protons
- Measured and monitored throughout the experiment.



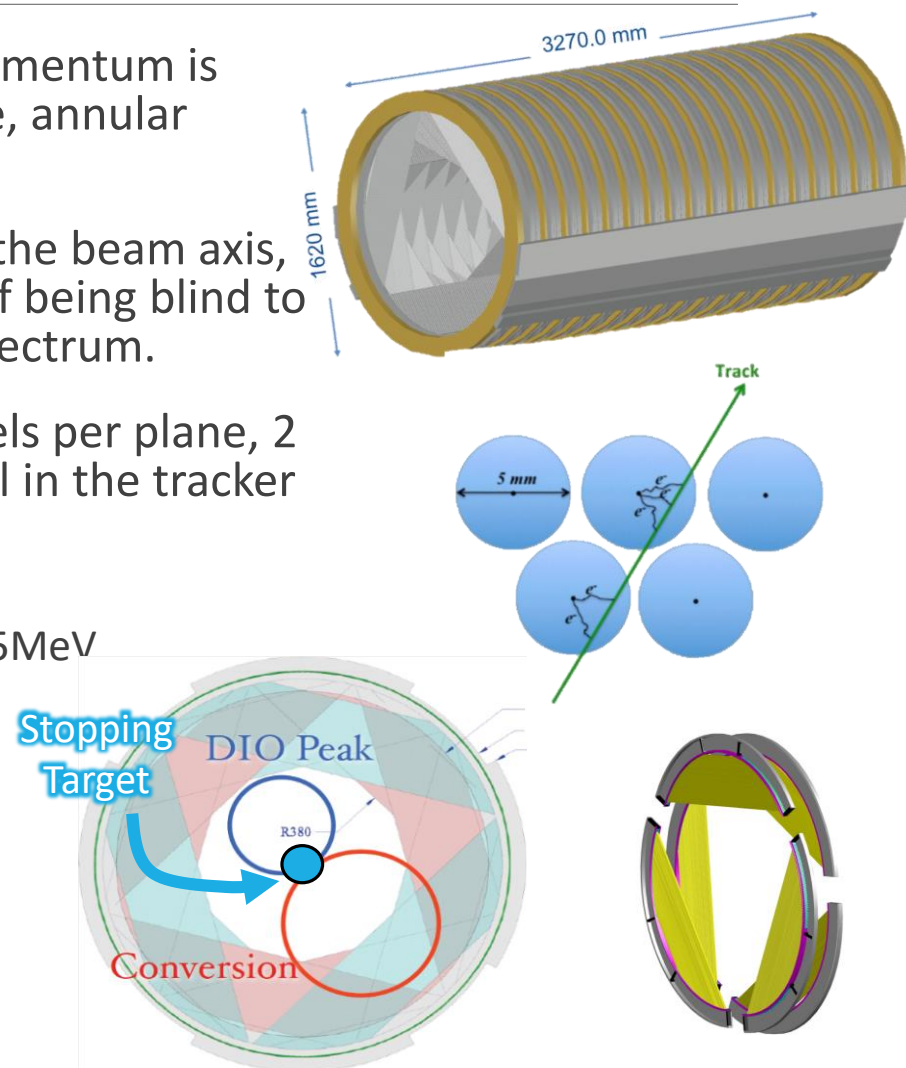
# Tracker

High-precision measurements of  $e^-$  momentum is made using a low-mass, straw drift tube, annular tracker, transverse to the beam axis.

Due to being un-instrumented close to the beam axis, the tracker has the distinct advantage of being blind to beam flash and next to all of the DIO spectrum.

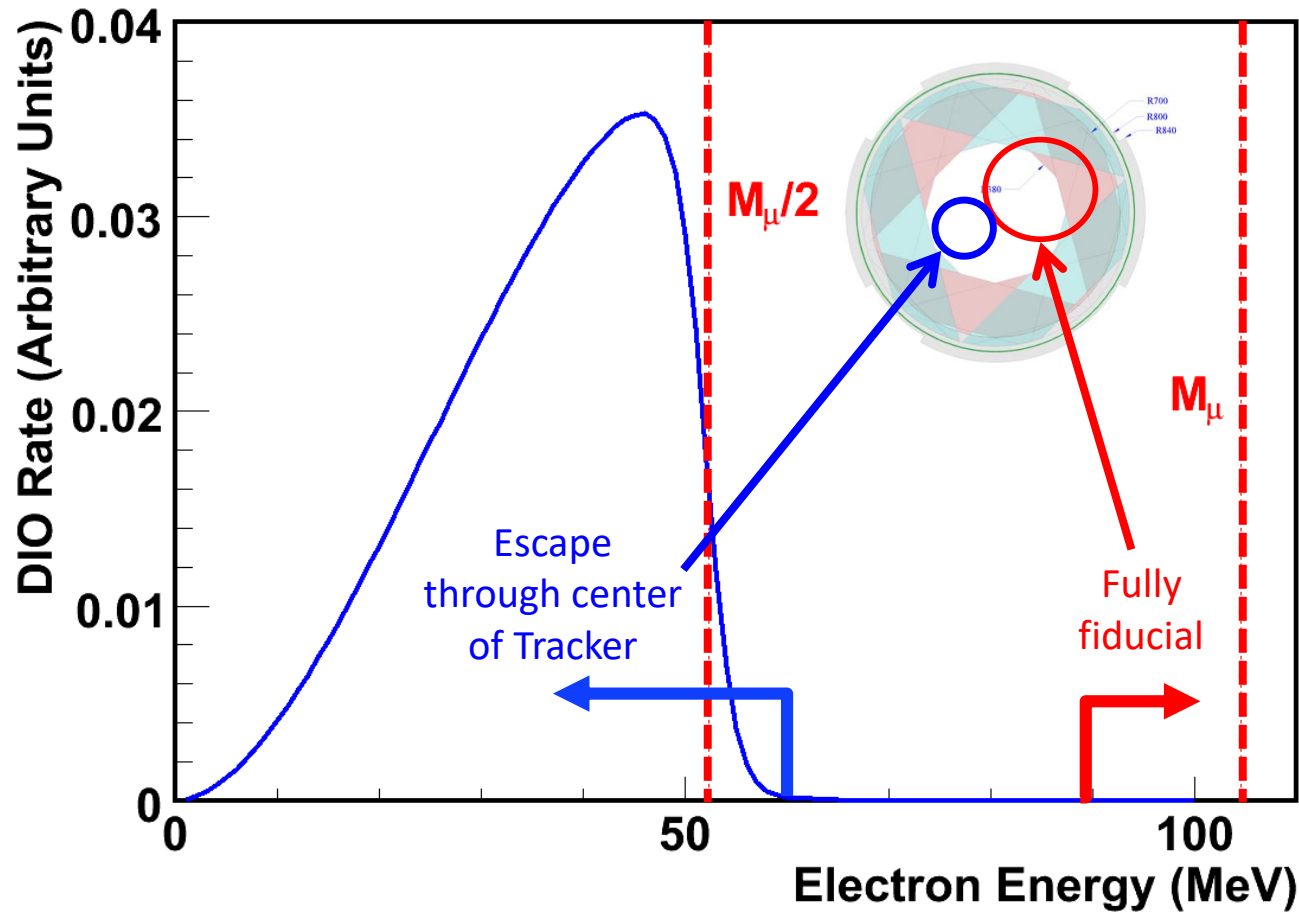
The tracker is built out of panels, 6 panels per plane, 2 planes per station, with 18 stations total in the tracker detector.

- Total 216 panels, ~21,000 straws
- Momentum Resolution  $< 200 \text{ KeV/c}$  @  $105 \text{ MeV}$
- $30^\circ$  rotation for stereo reconstruction
- 5 mm diameter straws
- $12 \mu\text{m}$  Mylar walls
- $25 \mu\text{m}$  tungsten wires
- Filled with  $\text{Ar}/\text{CO}_2$



# Tracker

Energy spectrum of electron emitted by muon decay in orbit



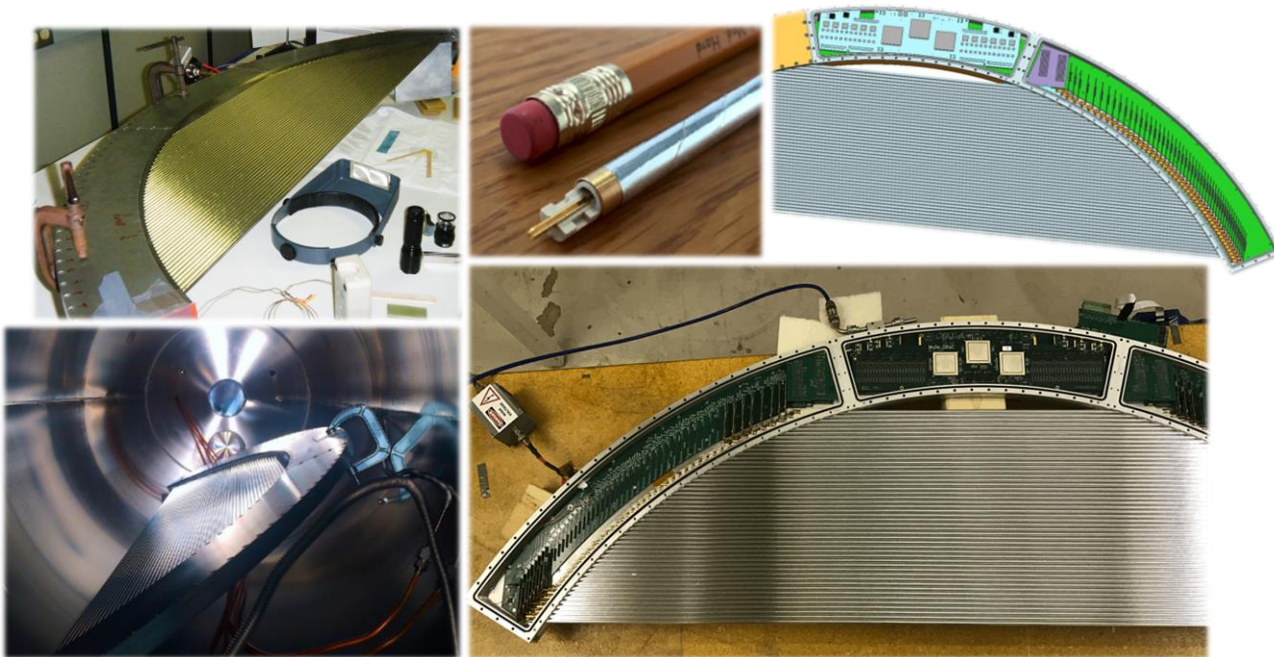
# Tracker

Several tracker panels have been built and tested using cosmic rays and a  $\text{Fe}^{55}$  source.

- Full plane assembled at Fermilab.

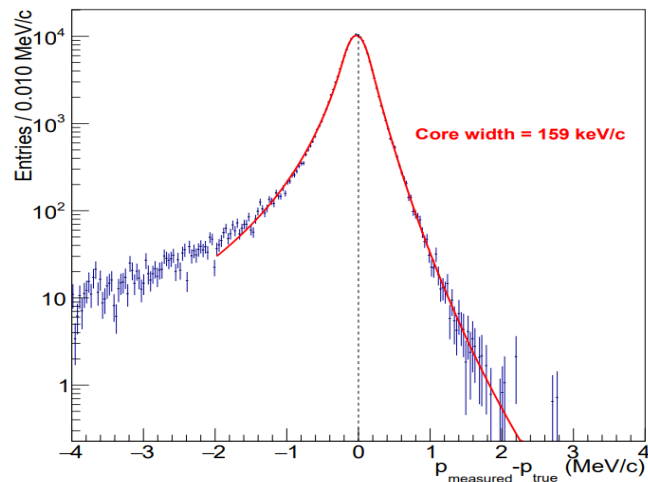
Panel assembly at the University of Minnesota (with Fermilab and U. Houston).

QA of panel components @ CUNY, Duke and LBL/UC Berkeley.

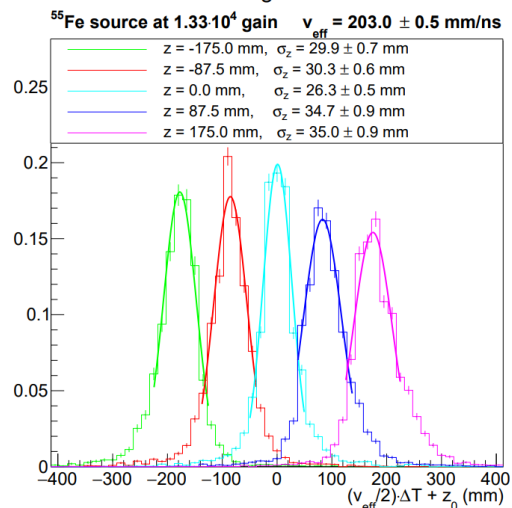


# Tracker

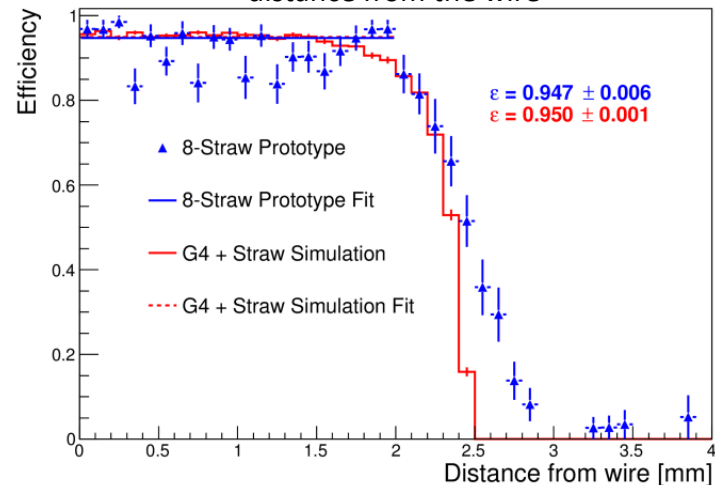
momentum resolution at start of tracker (simulation)



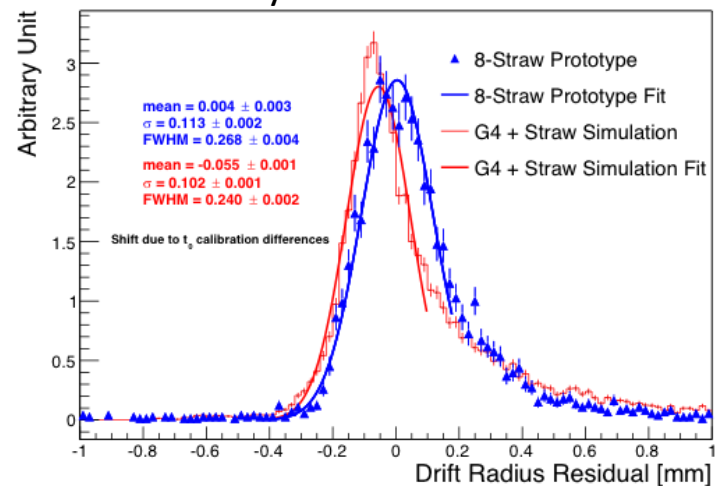
Mu2e Straw Longitudinal Resolution



Cosmic Rays: Straw hit efficiency as a function of the distance from the wire



Cosmic Rays: Transverse Resolution





# Calorimeter

A high-granularity crystal-based calorimeter will measure the energy of  $e^-$  coming out of the stopping target.

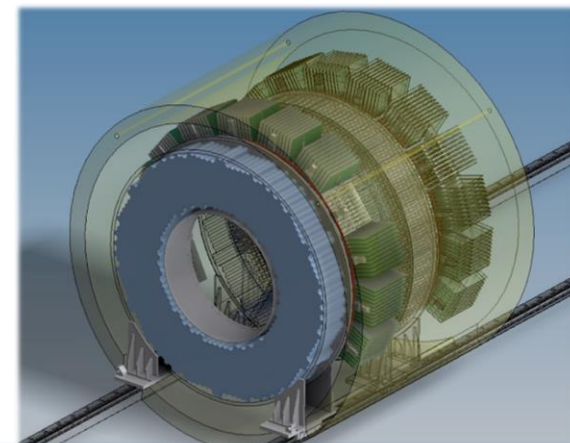
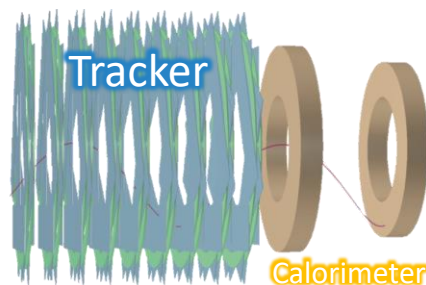
- This measurement is complementary to the Tracker's momentum measurement.

It provides:

- Precise timing  $\sigma_t \sim 100\text{ps}$
- Particle identification
- Seeds for the Tracker
  - Protection against pattern recognition errors in Tracker
- $\mu$  rejection x200 with 96%  $e^-$  efficiency

Comprised of 2 annuli of CsI crystal scintillators.

- Radiation Hard
- Good energy resolution  $\sigma_E/E \approx 5\% @ 105\text{MeV}$



1400 CsI  
Crystals  
 $3 \times 3 \times 20$   
 $\text{cm}^3$

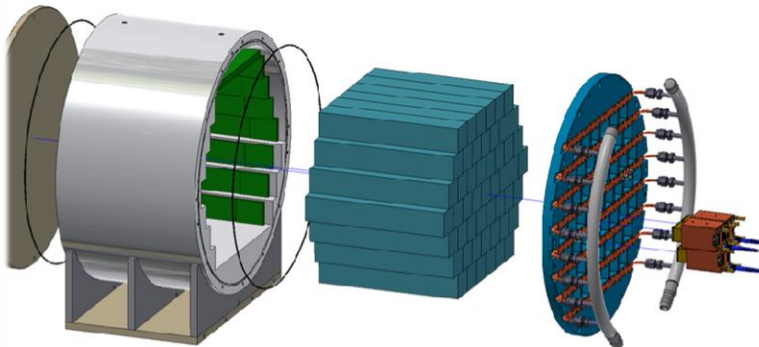
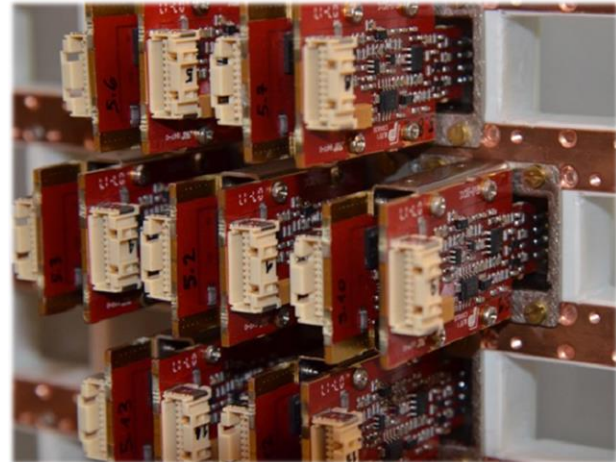
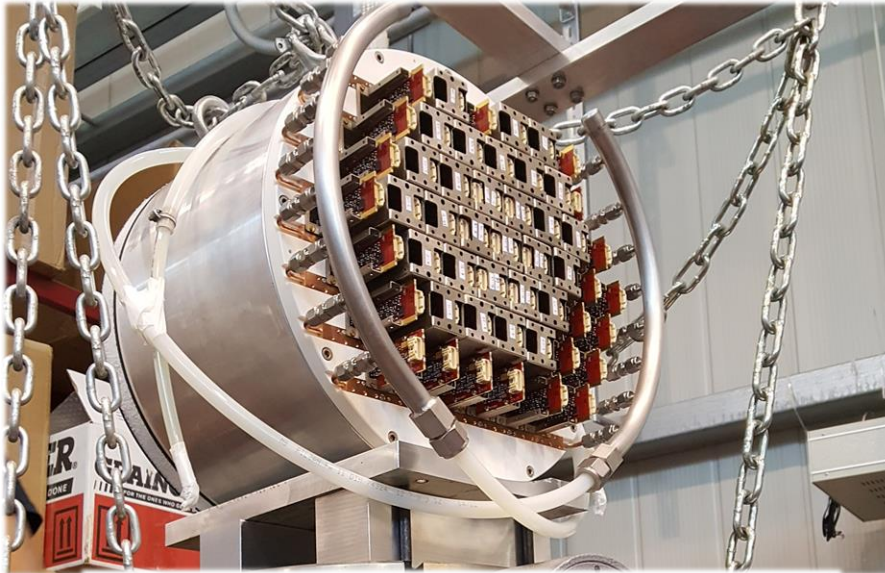
2800 SiPMs  
2 SiPMs  
per crystal

Disk Radii  
37-66cm

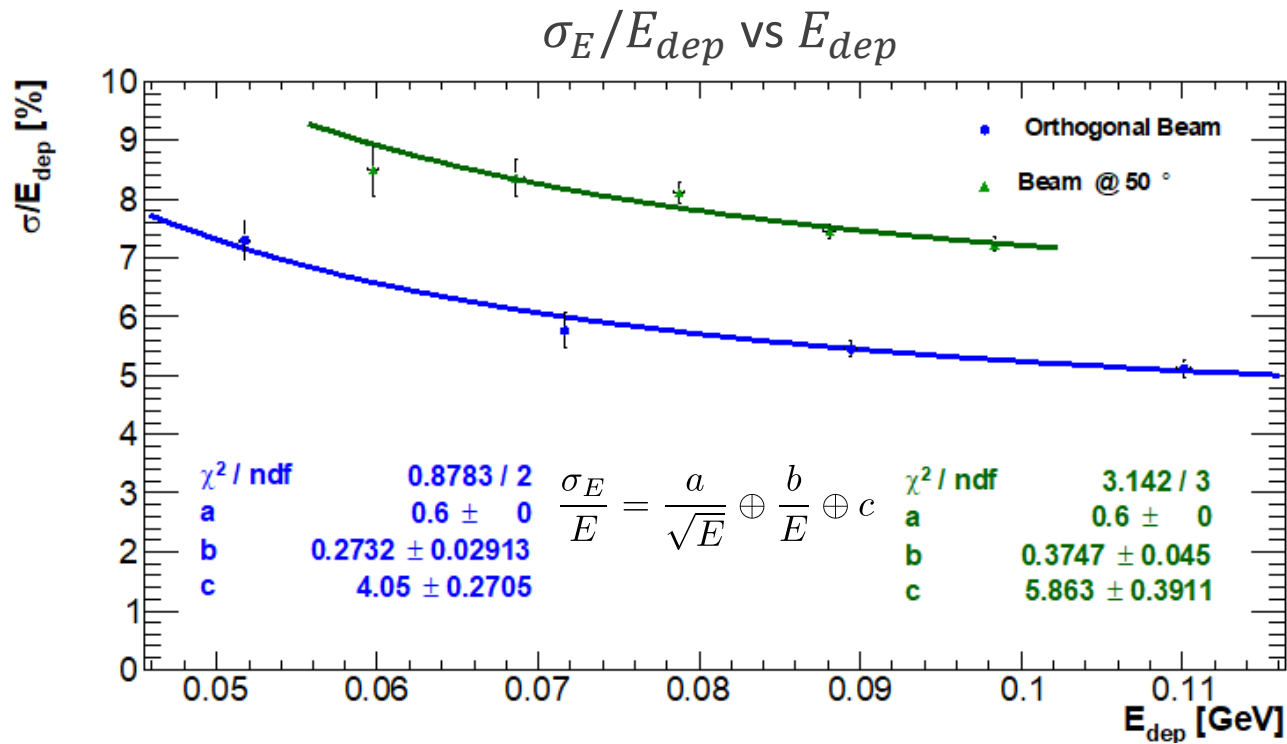


# Calorimeter

A fully-instrumented prototype calorimeter was built and tested.



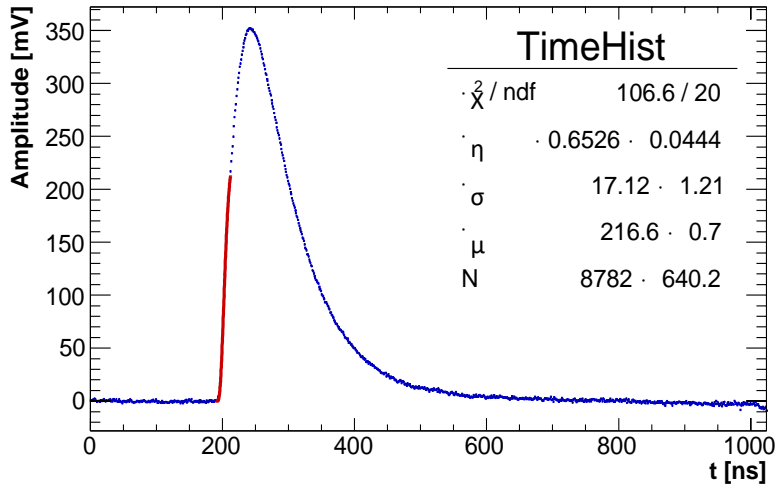
# Calorimeter



$$\frac{\sigma_E}{E_{dep}} \approx 5\% @ E_{beam} 100 \text{ MeV}$$

# Calorimeter

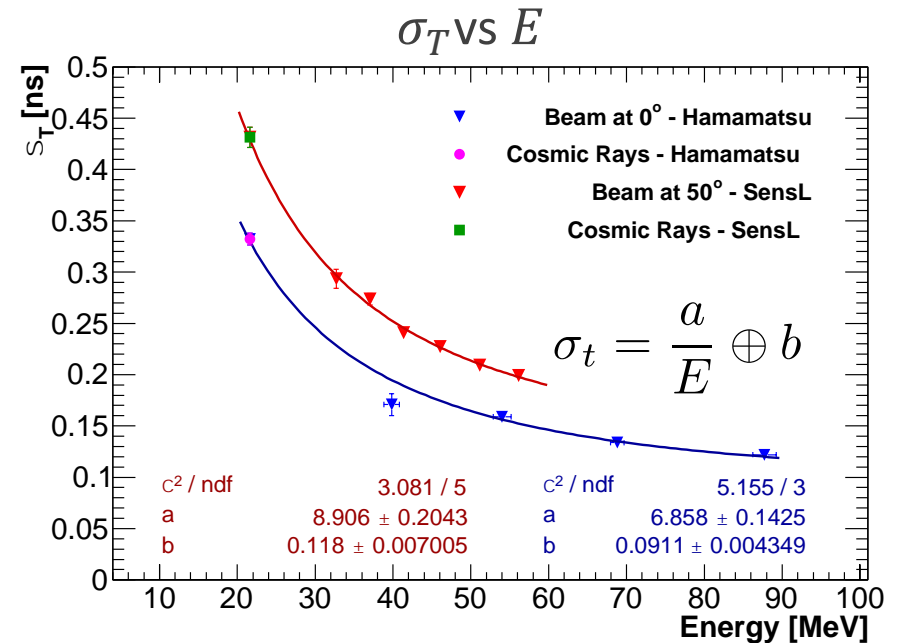
## Timing



$$\frac{\sigma_T(T_1 - T_2)}{\sqrt{2}} \sim 132 \text{ ps} @ E_{\text{beam}} = 100 \text{ MeV}$$

Log Normal fit on leading edge.

Constant Fraction method used CF = 5%.

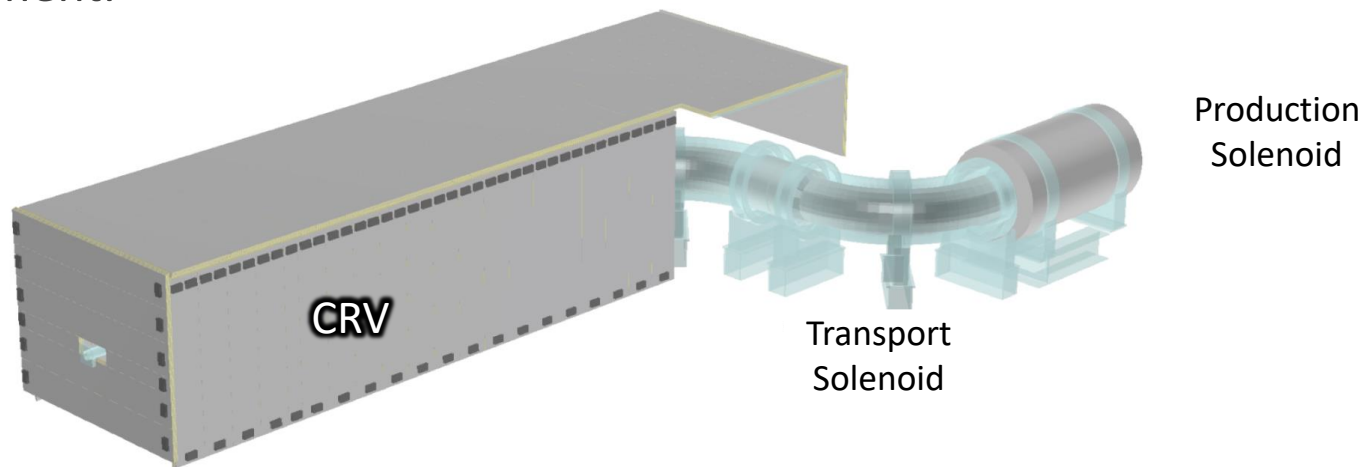


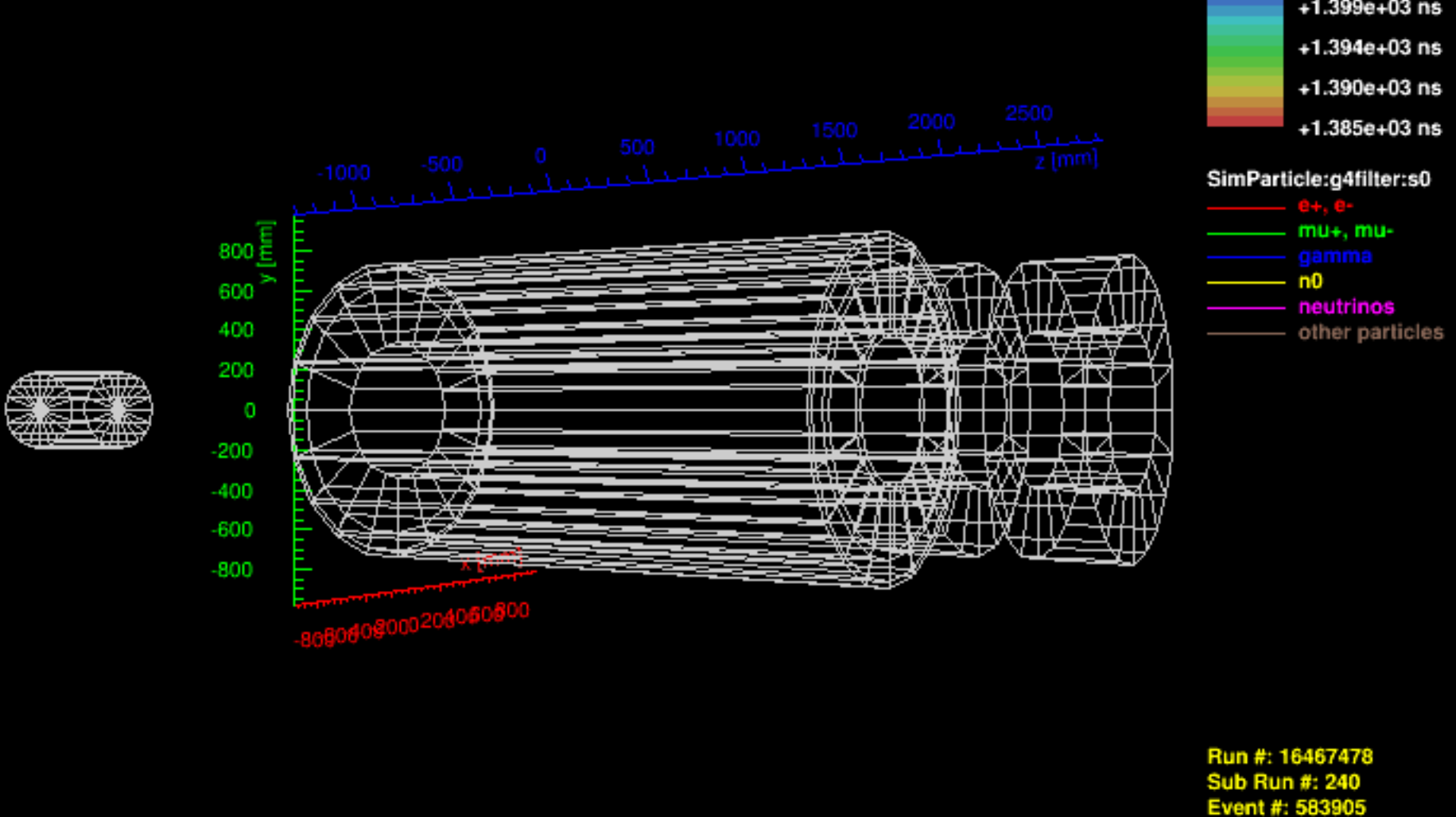
# Cosmic Ray Veto (CRV)

Cosmic rays infiltrating the experiment have the potential to create electrons and positrons through in-flight decays, as well as secondary interactions and delta-ray production in materials within the experiment's detector.

It is expected that one conversion-like event will occur per day, which can be suppressed by implementation of the CRV.

The CRV must have an overall efficiency of 99.99%, which limits the number of background events to 0.25 over the run time of the experiment.





# Conversion-like $e^-$ from Cosmic Rays

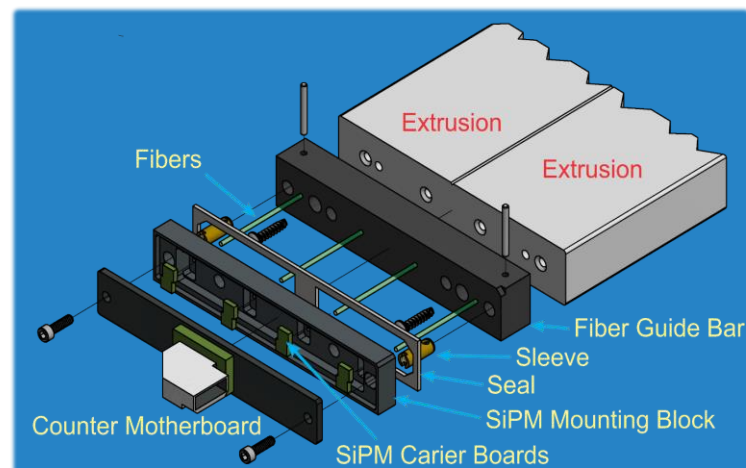
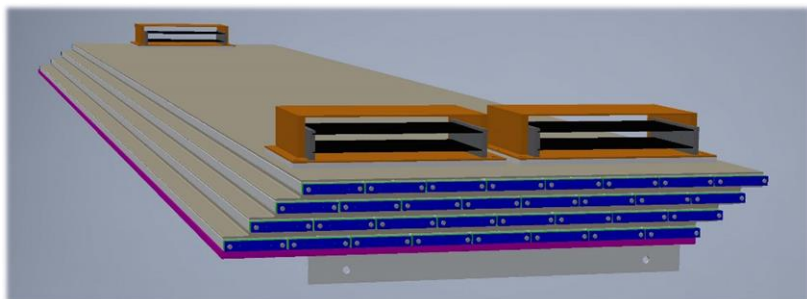
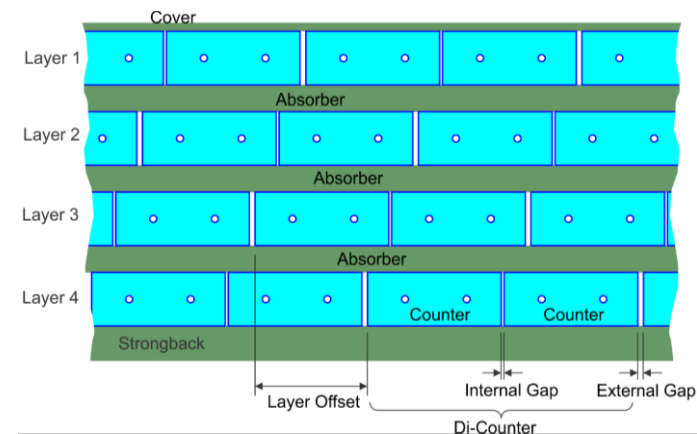
Cosmic rays entering the detector have the ability to create conversion-like electrons, faking muon-conversion signal.

The CRV will be active-shielding against the entrance of cosmic rays.

# Cosmic Ray Veto (CRV)

Four layers of extruded scintillator, read out by wavelength shifting fibers (WLS) and SiPMs, cover the entire detector solenoid and part of the transport solenoid.

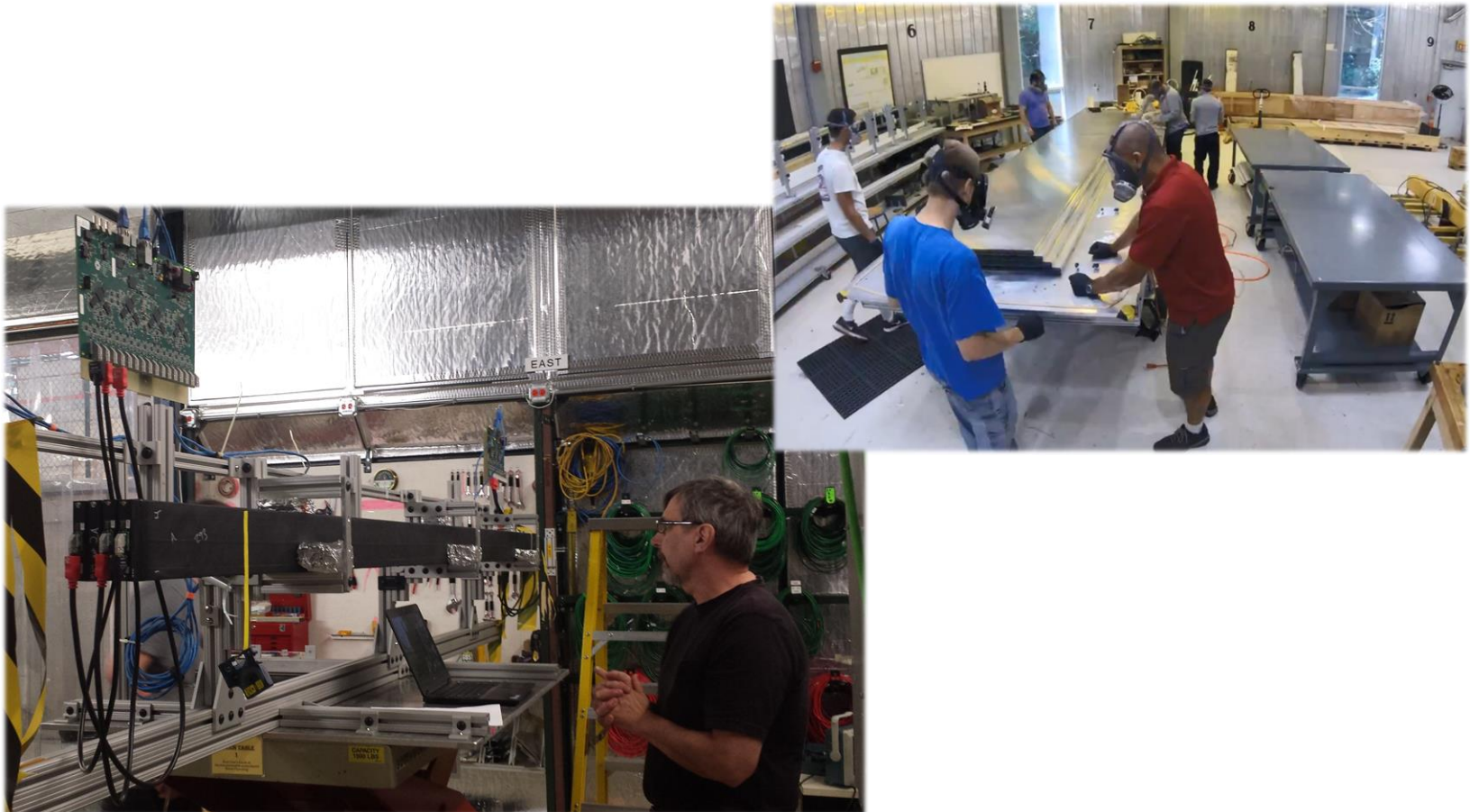
- Total coverage area of 391 m<sup>2</sup>
- Total mass of ~68,500 kg  $\cong$  75.5 tons
- 5,504 scintillator extrusions
- 52.7 km of WLS fibers
- 19,808 SiPMs
- 310 Front End Boards





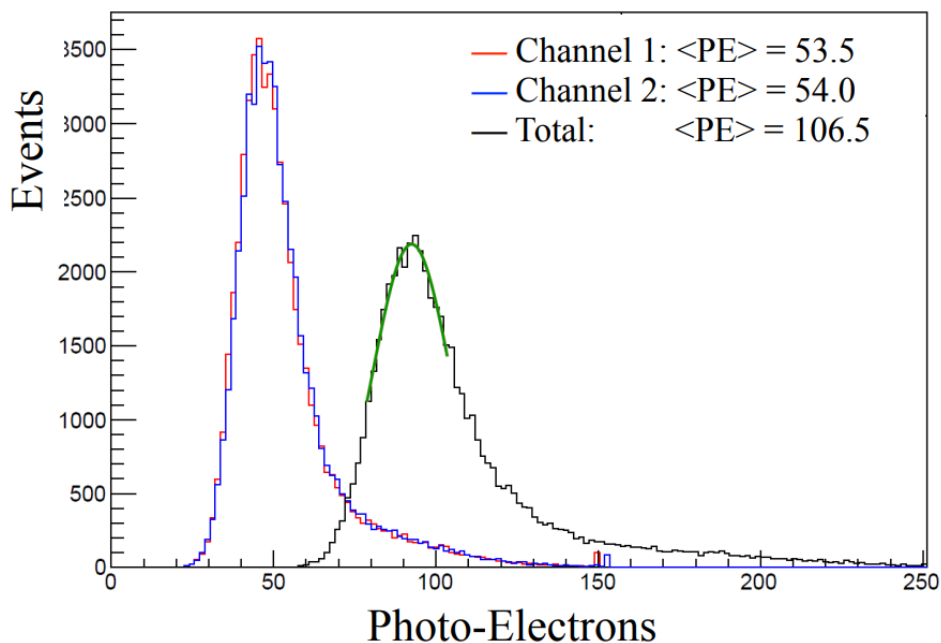
# Cosmic Ray Veto (CRV)

Three prototype, 4.5m-long detector modules and detector components have been built and tested.

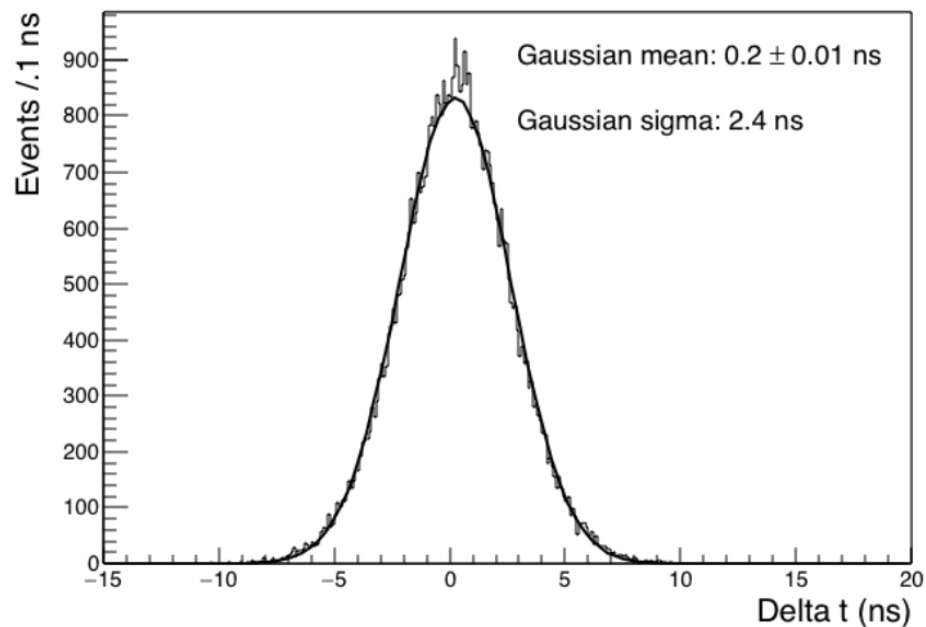


# Cosmic Ray Veto (CRV)

Photoelectron Yield @ 1m



Time Resolution

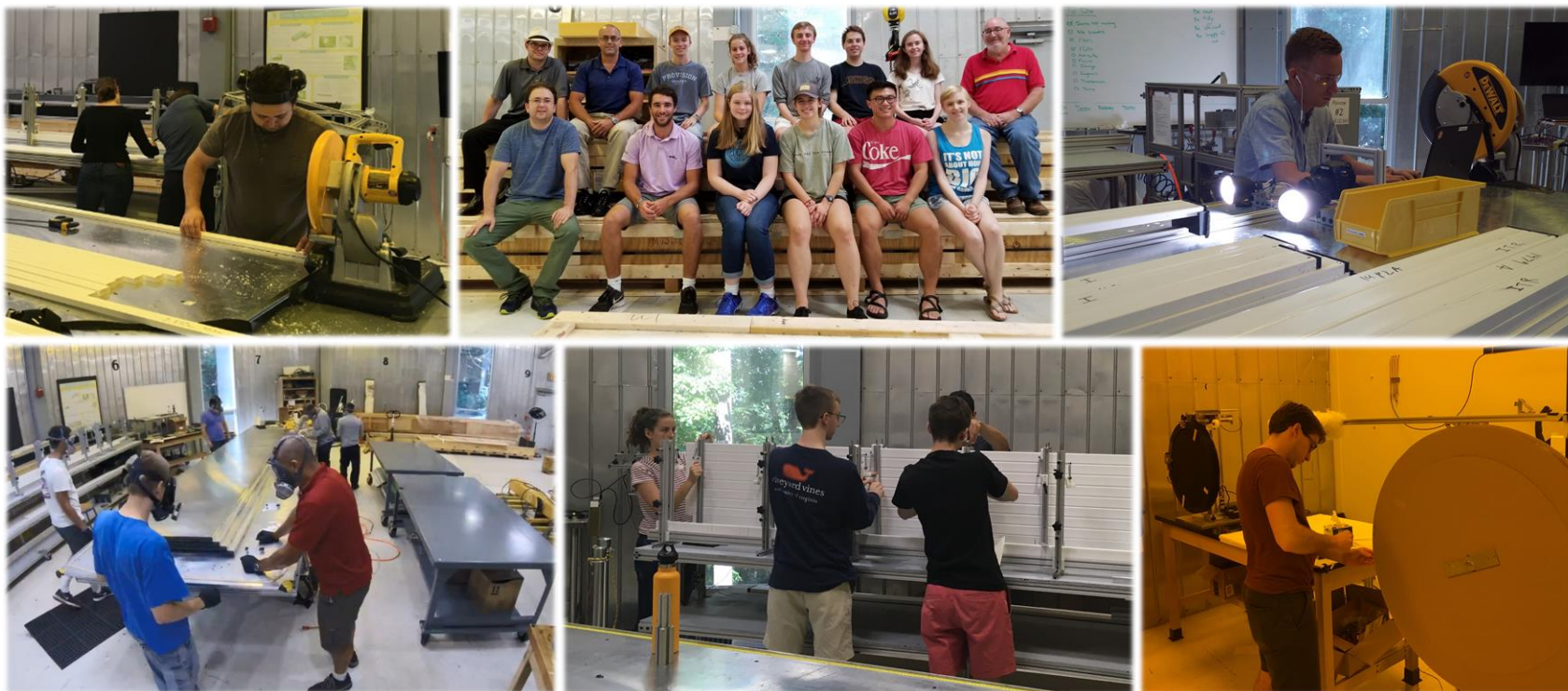


# Cosmic Ray Veto (CRV)

Currently being fabricated at the University of Virginia.

There are 5 CRV posters being presented in the poster session.

- Check them out!



# Status of Mu2e

Successfully passed DOE reviews.

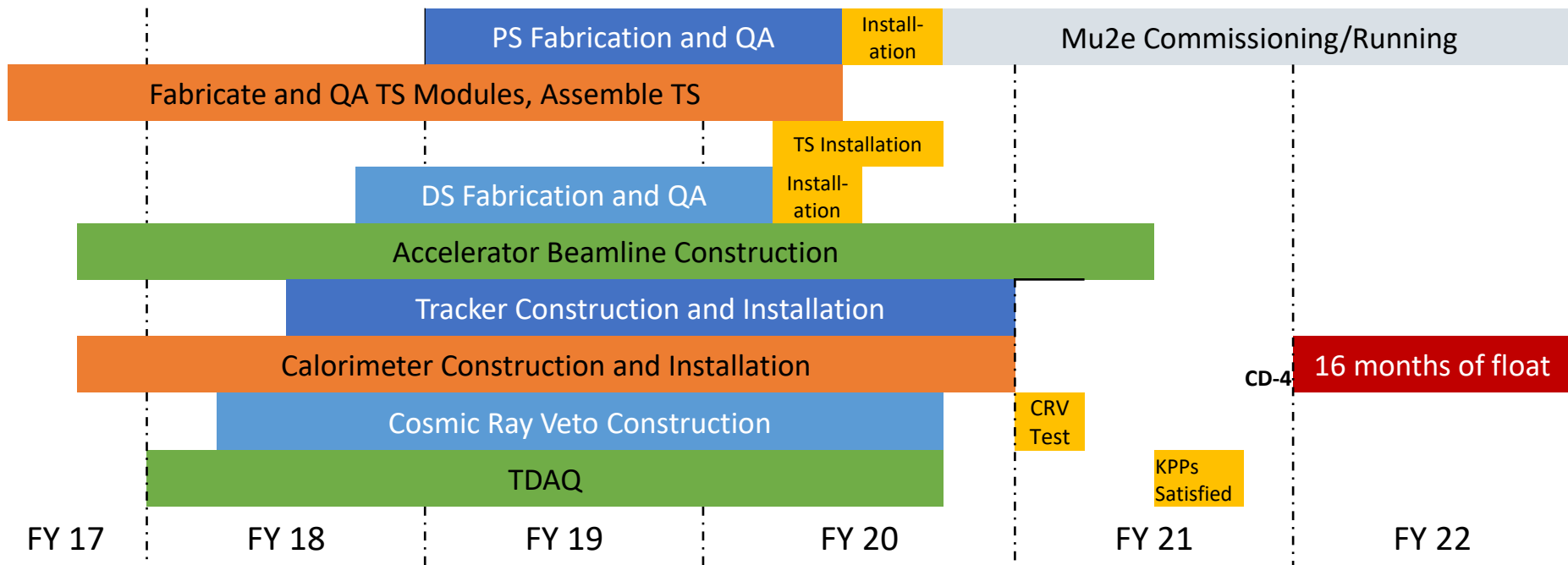
The detector hall construction has finished.

The various detectors are currently under construction.

Solenoid installation will begin in 2020.

Experiment commissioning will begin in 2020.

On track to begin taking data in 2022.





# Summary

---

Mu2e has excellent discovery potential and the ability to reveal BSM physics.

- Improvement in sensitivity by 4 orders of magnitude
- Probing of higher mass scales  $\mathcal{O}(10^4 \text{ TeV})$
- Sensitive to a wide range of BSM physics models
- Complementary to searches conducted by other experiments

The experiment is under construction and on schedule to begin commissioning in 2020.

Technical Design Report:

- <http://arXiv.org/abs/1501.05241>

Web site:

- <http://mu2e.fnal.gov>

